ELSEVIER

Physica D 81 (1995) 148–176

PHYSICA D

Global competition and local cooperation in a network of neural oscillators

David Terman [a], DeLiang Wang [b]

[a] *Department of Mathematics, The Ohio State University, Columbus, Ohio 43210, USA*

[b] *Laboratory of AI Research, Department of Computer and Information Science and Center for Cognitive Science, The Ohio State University, Columbus, Ohio 43210, USA*

Received 16 December 1993; revised 3 August 1994; accepted 30 September 1994

Communicated by C.K.R.T. Jones

Abstract

An architecture of locally excitatory, globally inhibitory oscillator networks is proposed and investigated both analytically and by computer simulation. The model for each oscillator corresponds to a standard relaxation oscillator with two time scales. Oscillators are locally coupled by a scheme that resembles excitatory synaptic coupling, and each oscillator also inhibits other oscillators through a common inhibitor. Oscillators are driven to be oscillatory by external stimulation. The network exhibits a mechanism of selective gating, whereby an oscillator jumping up to its active phase rapidly recruits the oscillators stimulated by the same pattern, while preventing the other oscillators from jumping up. We show analytically that with the selective gating mechanism, the network rapidly achieves both synchronization within blocks of oscillators that are stimulated by connected regions and desynchronization between different blocks. Computer simulations demonstrate the model's promising ability for segmenting multiple input patterns in real time. This model lays a physical foundation for the oscillatory correlation theory of feature binding and may provide an effective computational framework for scene segmentation and figure/ground segregation.

1. Introduction

A basic attribute of perception is its ability to group elements of a perceived scene or sensory field into coherent clusters (objects). This ability underlies perceptual processes such as figure/ground segregation, identification of objects, and separation of different objects, and it is generally known as scene segmentation or perceptual organization. Segmentation can be either peripheral or central. Peripheral segmentation is based on the correlation of local qualities within an input scene, and central segmentation is based on prior knowledge (memories) about the input scene. Despite the fact that humans perform it with apparent ease, the general problem of scene segmentation remains unsolved in the engineering of sensory processing, such as computer vision and auditory processing. As the technology of single-object recognition has become more and more advanced in recent years, the demand for a solution to scene segmentation is ever increasing since natural scenes are rarely composed of a single object.

Fundamental to scene segmentation is the grouping of similar sensory features and the segregation of dissimilar ones. Theoretical investigations of brain functions and perceptual organization point to the mech-

SSDI 0167-2789(94)00205-3

anism of temporal correlation as a representational framework [48,1,50]. The correlation theory of von der Malsburg [48] asserts that an object is represented by the temporal correlation of the firing activities of the scattered cells coding different features of the object. A natural way of encoding temporal correlation is to use neural oscillations [50], whereby each oscillator encodes some feature (maybe just a pixel, or picture element) of an object. In this scheme, each segment (object) is represented by a group of oscillators that shows synchrony (phase-locking with zero phase shift) of the oscillations, and different objects are represented by different groups whose oscillations are desynchronized from each other. Let us refer to this form of temporal correlation as *oscillatory correlation*. Evidently, the neurobiology of the brain provides the necessary means for implementing oscillatory correlation in the sense that neurons are spike generators, and brain waves are widespread in EEG recordings [23].

More recently, the theory of oscillatory correlation has received direct experimental support from cell recordings in the cat visual cortex [9,17]. The main points of these findings are: (1) Neural oscillations are triggered by sensory stimulation, known as stimulus-driven; (2) Global phase locking of neural oscillations with zero phase shift occurs when the stimulus is a coherent object (a long visual bar) or strongly correlated (the same location); (3) No phase locking exists across different stimuli if they are not related with each other. These basic findings have been confirmed by later experiments which demonstrated that phase locking can occur between the striate cortex and the extrastriate cortex [10], between the two striate cortices of the two brain hemispheres [11], and across the sensorimotor cortex in the monkey [37].

The discovery of synchronous oscillations in the visual cortex has triggered much interest from the theoretical community in simulating the experimental results (see among others [22,45,44,26,5,51]) and in exploring oscillatory correlation to solve the problems of scene segmentation and figure/ground segregation [55,3,46,18,49,36]. While several demonstrate synchronization in a group of oscillators using local (lateral) connections [26,43,51,52], most of these models rely on long range connections to achieve phase synchrony. It has been argued that local connections in reaching synchrony may play a fundamental role in scene segmentation since long-range connections would lead to indiscriminate segmentation [46,53]. More specifically, a network with long-range connections indiscriminately connects all the oscillators which are activated simultaneously by multiple objects, because the network is dimensionless and loses critical geometrical information about the objects. This point can be illustrated by Fig. 1 where three objects constitute the input scene. A human viewer can easily segment the three objects apart. In fact, when we said 'three objects', we already appealed to the reader's perceptual ability of segmenting the input into three connected objects. Yet this elementary task of scene segmentation cannot be performed by a network of all-to-all connections, because a unit representing a pixel in one object connects to the units representing the pixels of the same object in the same way as it does to units representing pixels of different objects. On the other hand, geometry is maintained in a locally connected oscillator network. A unit representing a pixel of one pattern does not connect to another unit representing a pixel of a different pattern, because the patterns are disconnected.

There are two aspects in the theory of oscillatory correlation: (1) synchronization within the same object and (2) desynchronization between different objects. Despite intensive studies on the subject, the question of desynchronization has been hardly addressed. In the simulations of von der Malsburg and Schneider [50], a global inhibitor was used to desynchronize two segments, each corresponding to a group of fully connected oscillators. Since their simulations involved a very small system and no analytic study was made, it is unclear how general their results are. It is often hidden in many previous studies that once synchrony is achieved within one object, desynchronization follows naturally since different objects are not synchronized. One needs to be more careful about this point. It is true that two objects are not correlated with each other if the two groups of oscillators behave independently. When a group reaches synchrony, it has a unique phase. But because the two groups are inde-

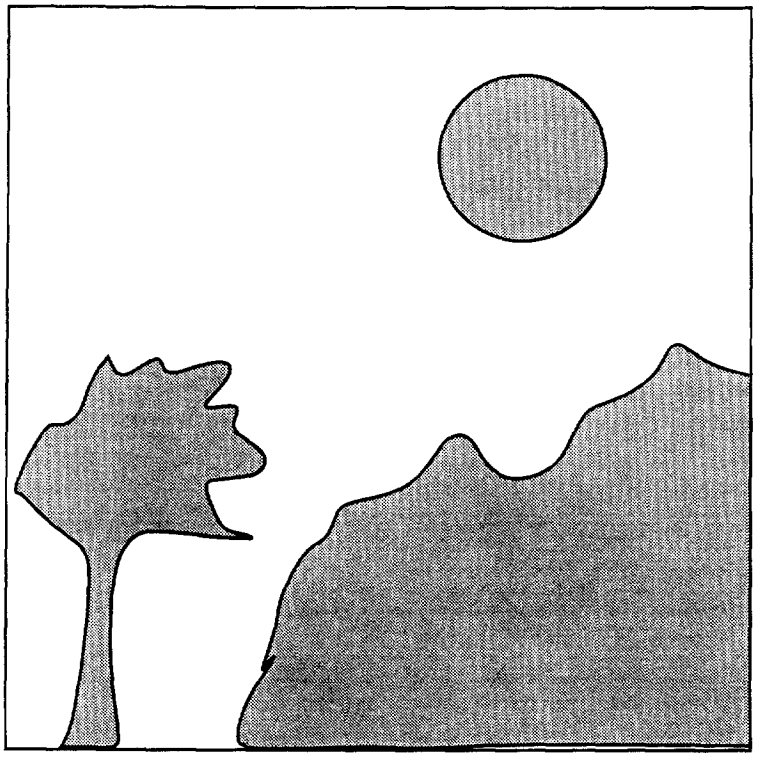

Fig. 1. A caricature of a visual image with three objects.

pendent, it is not guaranteed that the two corresponding phases are not close to each other so that the system would fail to separate them based on their phases. This problem can be avoided if one repeats segmentation trials so that on the average, the chances of accidentally aligning the phases of the two groups are greatly reduced. This is exactly what is used in many simulations (10 trials in [46,51]; 20 trials in [26]). Obviously, this proposal has the computational disadvantage of much increased overall time to complete a segmentation task. This concern becomes more severe by the following two factors. First, the synchrony within each segment is generally not perfect due to noise and the practical limitations on the time that is allowed for the system to reach synchrony. Imperfect synchrony requires certain tolerance of phase discrepancies within each group. This in turn makes the possibility of wrongly grouping two independent objects higher. Secondly, as the number of objects to be segmented increases, the chances of wrongly grouping two objects significantly increase. Another disadvantage of this proposal is that it makes scene segmentation in real time impossible.

In this article, we propose and analyze a novel mechanism for an oscillator network to rapidly achieve both grouping within each object and segmentation between a number of simultaneously presented objects. This mechanism is composed of the following elements: (1) A new model of a basic oscillator; (2) Local excitatory connections to produce phase synchrony within each group of oscillators representing the same object; (3) A global inhibitor that receives input from the entire network and feeds back with inhibition to produce desynchronization of the oscillator groups representing different objects. In other words, the mechanism consists of local cooperation and global competition, thus fully encoding oscillatory correlation. This surprisingly simple neural architecture may provide an elementary approach to scene segmentation and a computational foundation for per-

ceptual organization.

The model is described in the following section. In Section 3, we introduce the basic geometric approach to analyzing the solutions to the model. Simple networks are discussed in order to illustrate the roles played by excitation and by inhibition. A number of rigorous results are proved in Section 4. Computer simulations of a two-dimensional oscillator network are shown in Section 5, where rapid segmentation of multiple objects is illustrated. In Section 6, several aspects of the model are discussed, including its neural plausibility and its potential for offering a novel computational framework for scene segmentation. Finally, Section 7 concludes the paper.

2. Model description

The building block of our oscillator network, a single oscillator i, is defined in the simplest form as a feedback loop between an excitatory unit x_i and an inhibitory unit y_i:

$$x_i' = 3x_i - x_i^3 + 2 - y_i + \rho + I_i + S_i \tag{2.1a}$$

$$y_i' = \epsilon(\gamma(1 + \tanh(x_i/\beta)) - y_i) \tag{2.1b}$$

Here, ρ denotes the amplitude of a Gaussian noise term, I_i represents external stimulation to the oscillator, and S_i denotes the coupling from other oscillators in the network.

The purpose of introducing the noise term is twofold. First, it can test the robustness of the system. The second and perhaps more important purpose is that it plays an active role in separating different input patterns. This point will be discussed later.

The parameter ϵ is chosen to be small in both the numerics and the analysis. Then (2.1), without any coupling or noise, corresponds to a standard relaxation oscillator. The x-nullcline of (2.1), $\mathcal{C} \equiv \{(x,y) : x' = 0\}$, is a cubic curve, while the y-nullcline, $\mathcal{H} \equiv \{(x,y) : y' = 0\}$, is a sigmoid function as shown in Fig. 2. In Fig. 2a, $I > 0$. The nullclines intersect along the middle branch of the cubic, and (2.1) is *oscillatory*. It gives rise to a stable periodic orbit for all values of ϵ sufficiently small. The periodic solution alternates between silent and active phases of near steady state behavior. The parameter γ is introduced to control the relative times that the solution spends in these two phases as shown later. In Fig. 2b, $I < 0$. The nullclines now intersect at a stable fixed point, P_I, along the left branch of the cubic. In this case the system does not give rise to any periodic orbits. The parameter β is used to control the steepness of the sigmoid function.

The system (2.1) resembles the single neuron caricature model by FitzHugh [12] and Nagumo et al. [38]. However, the form of the nonlinearities in (2.1) and the parameter γ provide a dimension of flexibility missing from the FitzHugh–Nagumo equations. The system (2.1) also resembles the single cell conductance-based model of Morris and Lecar [35]. As discussed in Subsection 4.5, our analysis is quite general and applies to the Morris–Lecar equations. The main reason for introducing the model (2.1) is its simplicity. It clearly identifies the mathematical properties needed in a model for scene segmentation. We have identified precisely those parameters required for synchronization of oscillators within a given group and desynchronization of oscillators not in the same group. Other models, such as the Morris–Lecar model, have other parameters which play a similar role to those in (2.1). Our simulations show, however, that with everything else the same, this model takes about only half of the computing time compared to the Morris–Lecar model to generate similar behavior. The oscillator model (2.1) may also be interpreted as a mean field approximation to a network of excitatory and inhibitory neurons (see [4,16]).

To illustrate the detailed properties of an isolated single oscillator ($S_i = 0$), Fig. 3 shows its behaviors with different values for the parameters of external input I and γ. In Fig. 3a, different amounts of external input are applied to the oscillator. It can be seen that the oscillator reached a stable fixed point when I was chosen to be -0.02, corresponding to the case without external stimulation. The frequency of oscillation increased a little when I was systematically increased. Also the higher segment corresponding to the active phase widened while the lower segment corresponding to the silent phase narrowed as I increased. This

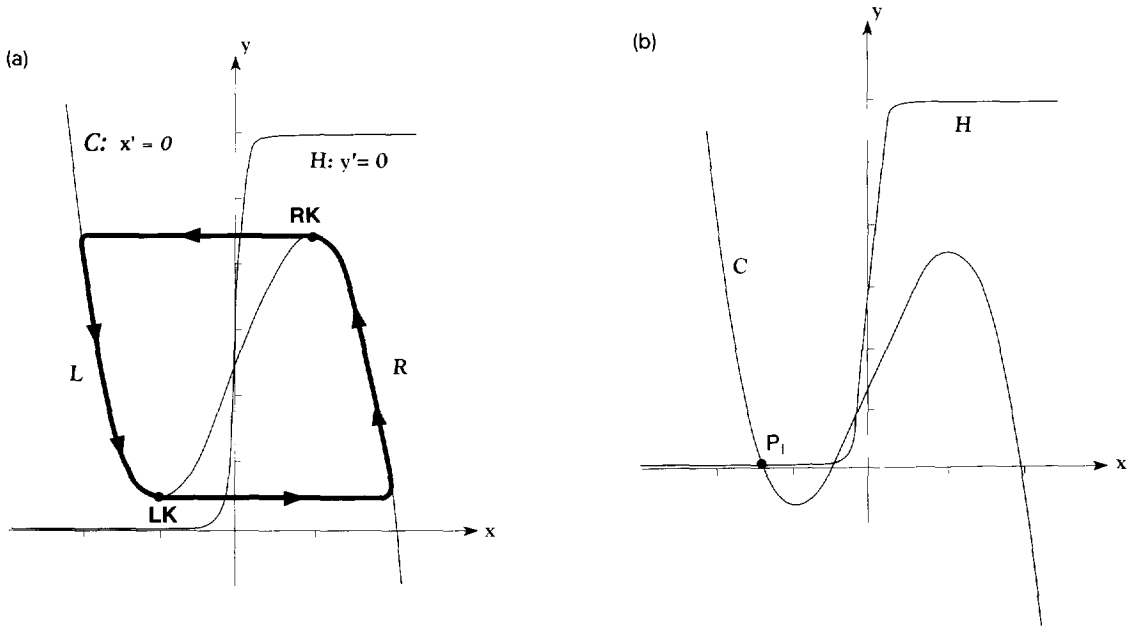

Fig. 2. Nullclines for a single oscillator. (a) If $I > 0$, then the system is oscillatory. The singular periodic orbit is shown with a bold curve. $\mathcal{L}$ and $\mathcal{R}$ are the left and right branches of the x-nullcline, respectively. The left and right knees of the cubic are labelled as LK and RK, respectively. (b) If $I < 0$, then there is no periodic solution. The fixed point P_I on the left branch of the cubic is asymptotically stable.

can be easily explained as follows. When I increases, the cubic is shifted upwards, and it gets nearer to the ceiling of the y-nullcline and farther away from the floor of the y-nullcline. Thus, the time that the periodic solution spends on the right branch becomes longer, while the time it spends on the left branch becomes shorter. For more detailed analysis see Sections 3 and 4. Fig. 3b shows the effects of varying γ. While the width of the lower segment changed little, the width of the higher segment was reduced substantially as γ increased. Again, this should be expected from the analysis since a larger γ raises the ceiling of the y-nullcline (see Fig. 2), which leads to a shorter time that the solution spends on the right branch of the cubic.

The architecture of the network that we study consists of a two dimensional matrix of oscillators plus a global inhibitor. Each oscillator in the network is connected to only its four neighboring oscillators, thus forming a 2D grid. This is the simplest form of local connections. As will be discussed later, lateral connections beyond immediate neighbors can enhance

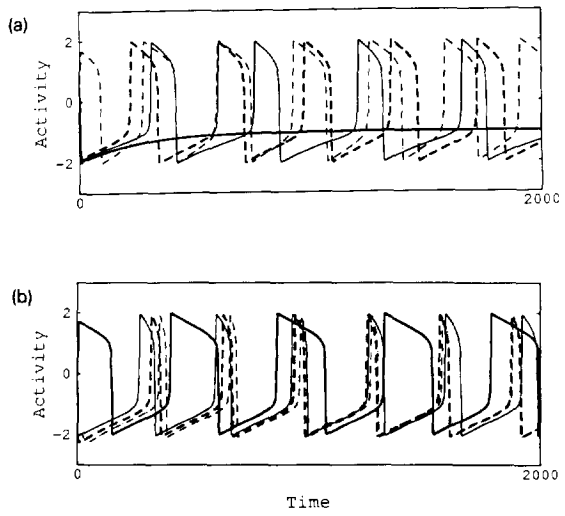

Fig. 3. (a) Effects of varying external input. Different curves are for different values of I respectively: Solid thick, $I = -0.02$; solid thin, $I = 0.4$; dashed thick, $I = 0.8$; dashed thin, $I = 1.6$. Parameter $\gamma = 4.0$. (b) Effect of varying γ. Solid thick, $\gamma = 3.0$; solid thin, $\gamma = 6.0$; dashed thick, $\gamma = 9.0$; dashed thin, $\gamma = 12.0$. Parameter $I = 0.8$. The other parameters are: $\rho = 0.02, \epsilon = 0.04, \beta = 0.1$. The simulation took 2,000 integration steps for each case.

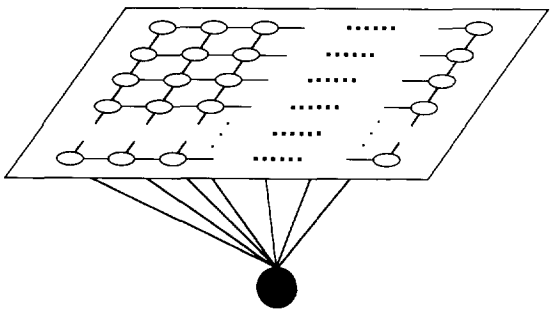

Fig. 4. Architecture of a two dimensional oscillator network with nearest-neighbor coupling. The global inhibitor receives an excitatory input from each oscillator of the network, and it in turn inhibits each oscillator. An oscillator is indicated by an empty circle, and the global inhibitor is indicated by the black circle.

the network's performance. The global inhibitor receives excitation from each oscillator of the grid and this, in turn, inhibits each oscillator. This architecture is shown in Fig. 4. The intuitive reason why this model gives rise to scene segmentation is the following. When multiple connected objects are mapped onto the grid, the local connectivity groups together the oscillators covered by each object. This grouping is reflected by phase synchrony within the oscillator group. The global inhibitor serves to desynchronize the oscillatory responses to different objects.

We assume that the coupling term S_i in (2.1) is given by

$$S_i = \sum_{k \in N(i)} W_{ik} S_\infty(x_k, \theta_x) - W_z S_\infty(z, \theta_{xz}) \qquad (2.2)$$

where

$$S_\infty(x, \theta) \equiv \frac{1}{1 + \exp\{-\kappa(x - \theta)\}} \qquad (2.3)$$

In (2.2), W_{ik} is a connection (synaptic) weight from oscillator k to oscillator i, and $N(i)$ is the set of neighboring oscillators that connect to oscillator i. In this model, $N(i)$ is the four immediate neighbors on the 2D grid, except on the boundaries where $N(i)$ may be either the two or three immediate neighbors. The parameter θ_x is a threshold above which an oscillator can effect its neighbors, and W_z is the weight of inhibition from the global inhibitor which we denote by z. The activity of the global inhibitor, also denoted by z, is given by

$$z' = \phi(\sigma_\infty - z) \qquad (2.4)$$

where $\sigma_\infty \equiv 0$ if $x_i < \theta_{zx}$ for every oscillator i, and $\sigma_\infty \equiv 1$ if $x_i \geq \theta_{zx}$ for at least one oscillator i. Hence, θ_{zx} represents a threshold. If the activity of every oscillator is below this threshold, then the global inhibitor will not receive any input. In this case $z \to 0$, and the oscillators will not receive any inhibition. If, on the other hand, the activity of at least one oscillator is above the threshold θ_{zx}, then the global inhibitor will receive input. In this case $z \to 1$, and each oscillator feels inhibition when z is above the threshold θ_{xz}. The parameter ϕ determines the rate at which the inhibitor reacts to such stimulation.

In summary, once an oscillator jumps to the active phase, it triggers the global inhibitor. This then inhibits the entire network as described in (2.2). On the other hand, an active oscillator spreads its activation to its nearest neighbors, again through (2.2), and from them to its further neighbors. Thus, the entire dynamics of the oscillator grid is a combination of local cooperation through excitatory coupling among neighboring oscillators and global competition via the global inhibitor. In Section 4, we prove a number of properties of this system.

3. Geometric description of solutions

3.1. Singular solutions

We take a very geometric approach to analyzing the solutions of (2.1)–(2.4). The solutions are viewed as trajectories in phase space, and ϵ is treated as a singular perturbation parameter. Much of the analysis is formal in the sense that we set $\epsilon = 0$ and then construct singular solutions of (2.1)–(2.4). The case $\epsilon > 0$ is considered in Subsection 4.5.

The singular solutions consist of two primary portions; these are the inner and outer solutions. An outer solution corresponds to when the solution exhibits near steady-state behavior. Outer solutions evolve on a slow time scale, and we derive a reduced system of equations from (2.1)–(2.4) which determines this slow evolution. Geometrically, an outer solution lies on an

invariant manifold of this reduced slow system.

Inner solutions correspond to rapid transitions between the near steady-state behavior. This portion of the singular solution evolves on a faster time scale than the outer solution, and we derive another reduced system of equations which determines this fast evolution. Geometrically, an inner solution corresponds to a trajectory in phase space which connects two invariant manifolds of the slow system.

In order to motivate the definition of a singular solution, we briefly discuss a single oscillator without any coupling or noise. That is, we consider the relaxation oscillator

$$x' = f(x,y) + I$$
$$y' = \epsilon g(x,y) \tag{3.1.1}$$

where $f(x,y) \equiv 3x - x^3 + 2 - y$ and $g(x,y) \equiv \gamma(1 + \tanh(x/\beta)) - y$.

If the nullclines, $\mathcal{C}$ and $\mathcal{H}$, intersect at a unique fixed point along the middle branch of $\mathcal{C}$, then there exists a stable periodic solution of (3.1.1) for all $\epsilon > 0$. This will be the case if $I > 0$ and β is sufficiently small. The singular solution of (3.1.1) with $I > 0$ is shown in Fig. 2a, and it consists of four pieces. The pieces that lie on $\mathcal{L}$ and $\mathcal{R}$ correspond to the silent and active phases, respectively. The slow system is obtained by introducing the slow time scale $\tau = \epsilon t$ in (3.1.1) and then setting $\epsilon = 0$ in the resulting equations. The inner solutions correspond to trajectories which connect $\mathcal{L}$ and $\mathcal{R}$. These are solutions of the fast system which is obtained by simply setting $\epsilon = 0$ in (3.1.1). One piece of the inner solution is when the oscillator 'jumps up'; this is a solution of the fast system which connects LK to $\mathcal{R}$. The other piece of the inner solution is when the oscillator 'jumps down'; this is a solution of the fast system which connects RK to $\mathcal{L}$.

In what follows, we assume that the parameter I takes one of two values. If the oscillator i (denoted by e_i) is stimulated, then $I_i \equiv I^+ > 0$, while if e_i is not stimulated, then $I_i \equiv I^- < 0$. Hence, the stimulated oscillators, without noise or coupling, are oscillatory, while the unstimulated oscillators do not oscillate.

We now define what is meant by a singular solution in the general case when there is coupling. We assume that all of the oscillators are identical, and the differential equations corresponding to a particular oscillator, say e_i, are (cf. (2.2))

$$x_i' = f(x_i,y_i) + I_i + \sum_{k\in N(i)} W_{ik} S_\infty(x_k,\theta_x) - W_z S_\infty(z,\theta_{xz})$$
$$y_i' = \epsilon g(x_i,y_i) \tag{3.1.2}$$

To simplify the discussion, we assume that the function $S_\infty(x,\theta)$ assumes the values 0 or 1. That is, $S_\infty(x,\theta) \equiv 0$ if $x < \theta$, and $S_\infty(x,\theta) \equiv 1$ if $x \geq \theta$. There is no problem in extending the analysis to the case when S_∞ is defined by (2.3) if the parameter κ is sufficiently large.

We do not include noise in (3.1.2), because this simplifies the analysis that follows. However our numerical studies clearly indicate that some degree of noise not only does not disrupt the behavior but also enhances the segmentation process. This point will be discussed later in Subsection 4.4 (see Remark 4.4b).

As before, the slow system is obtained by introducing the slow time scale $\tau = \epsilon t$ in (3.1.2) and then setting $\epsilon = 0$ in the resulting system. This yields the system

$$0 = f(x_i,y_i) + I_i + \sum_{k\in N(i)} W_{ik} S_\infty(x_k,\theta_x) - W_z S_\infty(z,\theta_{xz})$$
$$y_i' = g(x_i,y_i) \tag{SS}$$

Note that the solution of the first equation in (SS) is a vertical translate of the cubic $\mathcal{C}$.

The parameters θ_x, θ_{zx}, and θ_{xz} are chosen so that $\theta_x < \theta_{zx}$ and $\theta_{xz} \in (0,1)$. We also assume that if e_i is in its silent phase, then $x_i < \theta_x$ so that $S_\infty(x_i,\theta_x) = 0$, while if e_i is in its active phase, then $\theta_{zx} < x_i$, so that $S_\infty(x_i,\theta_x) = 1$.

The slow equation for the inhibitor is $z \equiv \sigma_\infty$. Hence, if all of the oscillators are in their silent phases, then $z = \sigma_\infty \equiv 0$ and $S_\infty(z,\theta_{xz}) = 0$. If at least one oscillator is active, then $z = \sigma_\infty \equiv 1$.

The fast system is obtained by simply setting $\epsilon = 0$ in (3.1.2). This yields the following system for e_i:

$$x_i' = f(x_i, y_i) + I_i + \sum_{k \in N(i)} W_{ik} S_\infty(x_k, \theta_x) - W_z S_\infty(z, \theta_{xz})$$
$$y_i' = 0 \qquad \text{(FS)}$$

The fast equation for the inhibitor is

$$z' = \phi(\sigma_\infty - z) \qquad (\text{FS}_I)$$

The cubics correspond to fixed points of (FS). The left and right branches of these cubics are the stable fixed points of (FS). Note that during an inner solution, when the oscillators jump between branches, the variables $S_\infty(x_k, \theta_x)$, $S_\infty(z, \theta_{xz})$ and σ_∞ may switch between 0 and 1.

We now define precisely what is meant by a singular solution. It is a continuous curve in phase space which is the union of smooth pieces. We parameterize this curve by the variable η. Suppose that there are N oscillators and let $e_i = (x_i(\eta), y_i(\eta)), i = 1, \ldots, N$. Then $\psi(\eta) = (e_1(\eta), e_2(\eta), \ldots, e_N(\eta), z(\eta))$ is a singular solution of (2.1)–(2.4) if it defines a continuous curve in phase space, and there exist $0 = \eta_0 < \eta_1 < \ldots$ such that

(i) if $\eta_{2j} < \eta < \eta_{2j+1}$, $j = 0, 1, \ldots$, then each $e_i(\eta)$ corresponds to a solution of (SS). Moreover, if $x_i(\eta) < \theta_{zx}$ for each i, then $z(\eta) = 0$. If $x_i(\eta) \geq \theta_{zx}$ for some i, then $z(\eta) = 1$.

(ii) Suppose that $\eta_{2j-1} < \eta < \eta_{2j}$, $j = 1, 2, \ldots$. Then each e_i corresponds to a solution of (FS) and z corresponds to a solution of (FS_I).

(iii) If $\eta = \eta_{2j-1}$, $j = 1, 2, \ldots$, then at least one of the oscillators is at one of the knees.

We conclude this section with some further notation. For $W_a \geq 0$ and $W_b \geq 0$, let $\mathcal{C}(W_a, W_b) \equiv \{(x, y) : f(x, y) + I + W_a - W_b = 0\}$. Let

$$\mathcal{C} = \mathcal{C}(0, 0) \quad \text{and} \quad \mathcal{C}_Z = \mathcal{C}(0, W_z)$$

Denote the left branches of $\mathcal{C}$ and $\mathcal{C}_Z$ by

$$\mathcal{L} = \{(x, y) : x = h(y)\} \quad \text{and}$$
$$\mathcal{L}_Z = \{(x, y) : x = h_Z(y)\},$$

respectively, where h and h_Z are smooth, decreasing functions. Denote the left knee of $\mathcal{C}$ by $LK = (x_L, y_L)$ and the right knee of $\mathcal{C}_Z$ by $RK_Z = (X_Z, Y_Z)$.

It follows that the slow system on $\mathcal{L}$ is given by

$$x = h(y)$$
$$y' = g(h(y), y) \equiv G(y) \qquad (\text{SS}_L)$$

This determines the slow evolution of each oscillator when every oscillator is in its silent phase. The slow system on $\mathcal{L}_Z$ is given by

$$x = h_Z(y)$$
$$y' = g(h_Z(y), y) \equiv G_Z(y) \qquad (\text{SS}_Z)$$

This determines the slow evolution of an oscillator in the silent phase when some other oscillator is in its active phase.

Choose W_m and W_M so that $W_m \leq W_{ik} \leq W_M$ for every weight W_{ik}. Note that

$$W_m \leq \sum_{k \in N(i)} W_{ik} \leq 4W_M \qquad (3.1.3)$$

for each oscillator e_i and all time. Denote the cubics $\mathcal{C}(W_m, W_z)$ and $\mathcal{C}(4W_M, W_z)$ by $\mathcal{C}_m$ and $\mathcal{C}_M$, respectively. Assume that the right knees of these cubics are at $RK_m = (X_m, Y_m)$ and $RK_M = (X_M, Y_M)$, respectively, and the left knee of $\mathcal{C}_m$ is at $LK_m = (x_m, y_m)$. We assume that $W_z < W_m$. This implies that $\mathcal{C}_m$ lies above $\mathcal{C}$. These cubics, together with their left and right branches and knees are shown in Fig. 5.

For $W > 0$, denote the right branch of the cubic $\mathcal{C}(W, W_z)$ by $\mathcal{R}_W = \{(x, y) : x = H_W(y)\}$, where H_W is a smooth, decreasing function. Then the slow system on $\mathcal{R}_W$ is given by

$$x = H_W(y)$$
$$y' = g(H_W(y), y) \equiv G_W(y) \qquad (\text{SS}_W)$$

Let $\psi_L(y, t)$ be the solution of the second equation in (SS_L) which satisfies $\psi_L(y, 0) = y$. If $y_1 < y_2$, define $\tau_L(y_1, y_2)$ by $\psi_L(y_2, \tau_L(y_1, y_2)) = y_1$. That is, $\tau_L(y_1, y_2)$ is the time of excursion from y_2 to y_1. Define $\psi_Z(y, t)$ and $\tau_Z(y_1, y_2)$ in a similar manner. Let $\Psi_W(y, t)$ be the solution of the second equation in (SS_W) which satisfies $\Psi_W(y, 0) = y$. If $y_1 < y_2$, define $\tau_W(y_1, y_2)$ by $\Psi_W(y_1, \tau_W(y_1, y_2)) = y_2$.

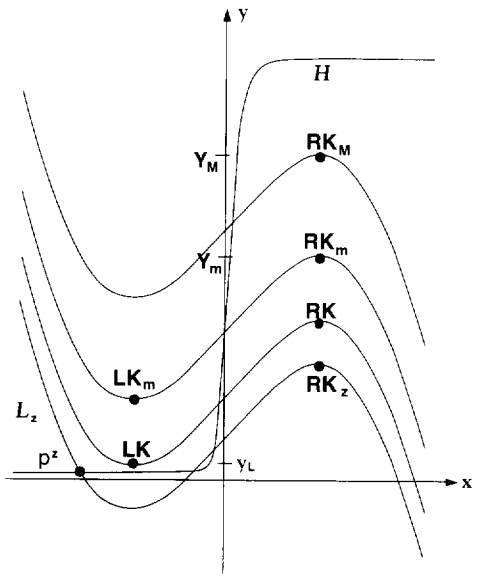

Fig. 5. Nullclines of the system (SS). If all the oscillators are silent, then they lie on $\mathcal{L}$. If an oscillator is silent, but another is active, then it lies on $\mathcal{L}_Z$. During its active phase, an oscillator which receives input lies on the right branch of a cubic between C_m and C_M.

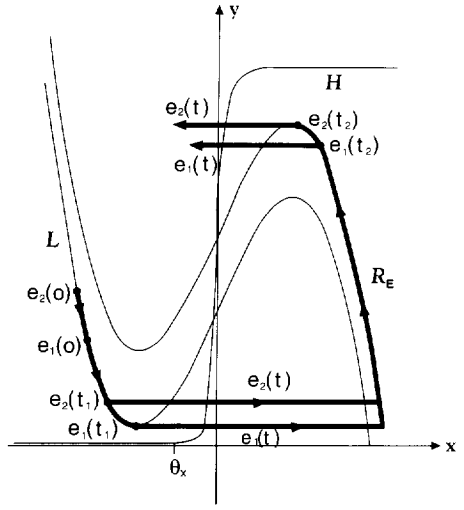

Fig. 6. Two oscillators coupled through mutual excitation. When e_1 jumps up at time $t = t_1$, the cubic corresponding to e_2 raises from C to C_E. This allows e_2 to jump up. When e_2 jumps down at $t = t_2$, the cubic corresponding to e_1 lowers from C_E to C. This allows e_1 to jump down.

3.2. *Simple networks*

We now consider two simple networks in order to illustrate the role played by excitation in synchronizing oscillators representing the same pattern, and the role played by inhibition in desynchronizing oscillators representing different patterns. We assume here that each oscillator is stimulated. Hence, each oscillator, without coupling or noise, is oscillatory with $I_i = I^+$.

We first consider the following network in which we do not include inhibition:

$$e_1 \rightleftharpoons e_2$$

We assume that $W_{12} = W_{21}$. The discussion here is similar to that given in Somers and Kopell [43] who introduced the notion of *fast threshold modulation*.

Assume that $e_1 = (x_1, y_1)$ and $e_2 = (x_2, y_2)$ begin, when $t = 0$, along $\mathcal{L}$. The singular solution is then shown in Fig. 6 for the case in which e_1 is sufficiently close to e_2. As in the case for one oscillator, the singular solution consists of several pieces. The first piece is when both oscillators move along $\mathcal{L}$ and satisfy (SS_L). This corresponds to the silent phase and lasts until one of the oscillators, say e_1, reaches the left knee LK. Suppose that e_1 reaches the left knee at $t = t_1$. Here, we consider the slow time scale. Note that with respect to the slow time variable, the jumps between the silent and active phases are instantaneous.

The second piece of the singular solution begins when e_1 jumps up. During the first part of this transition, e_1 satisfies (FS) with $S_\infty(x_2, \theta_x) = S_\infty(z, \theta_{xz}) = 0$ together with the boundary condition $lim_{t\to-\infty}(x_1(t), y_1(t)) = LK$. When $x_1(t)$ crosses θ_x, $S_\infty(x_1, \theta_x)$ switches from 0 to 1. This 'raises' the cubic corresponding to e_2 from C to another cubic which we denote by C_E. Let LK_E and RK_E denote the left and right knees of C_E. If $|y_1 - y_2|$ is sufficiently small, then e_2 lies below LK_E, and e_2 jumps up.

The third piece of the singular solution is when both oscillators lie on $\mathcal{R}_E$, the right branch of C_E, and evolve according to (SS) with $S_\infty(x_1, \theta_x) = S_\infty(x_2, \theta_x) = 1$ and $S_\infty(z, \theta_{xz}) = 0$. Note that, in some sense, the ordering in which the oscillators track along the slow manifolds is now reversed. While the oscillators moved 'down' $\mathcal{L}$, e_1 was ahead of e_2. When the oscillators move 'up' $\mathcal{R}_E$, e_2 leads the way. The oscillators remain on $\mathcal{R}_E$ until one of the oscillators, in this case

e_2, reaches RK_E. In Fig. 6, we show this to be at the slow time $t = t_2$.

The next piece of the singular solution is when the oscillators jump down to the silent phase. At first e_2 jumps down. When $x_2(t)$ crosses θ_x, $S_\infty(x_2, \theta_x)$ switches from 1 to 0. This lowers the cubic corresponding to e_1 from C_E to C. If, at this time, e_1 lies above RK, then e_1 jumps down to the silent phase. Once both oscillators lie on $\mathcal{L}$ again, the entire process repeats itself.

We next consider the network:

$$e_1 \rightleftharpoons z \rightleftharpoons e_2$$

Here, e_1 and e_2 are oscillators without direct excitatory coupling and z is the global inhibitor. Hence, e_1 and e_2 correspond to separate patterns. We assume that e_1 and e_2 both begin in their silent phases with $y_1 \neq y_2$. When one of the oscillators, say e_1, jumps up, then the inhibition has the effect of lowering the cubic corresponding to e_2. This prevents e_2 from firing at least until e_1 returns to the silent phase.

The singular solution is shown in Fig. 7. Both oscillators begin on $\mathcal{L}$ with $y_1 < y_2$. They track along $\mathcal{L}$ according to (SS_L) until e_1 reaches LK. Suppose that this is at $t = t_1$, where, as before, we consider the slow time scale. When both oscillators lie on $\mathcal{L}$, $z = 0$. The second piece of the singular solution corresponds to when e_1 jumps up. When x_1 crosses θ_{zx}, σ_∞ switches from 0 to 1. Hence, z satisfies (FS_Z) and $z \to 1$ on the fast time scale. When z crosses θ_{xz}, $S_\infty(z, \theta_{xz})$ switches from 0 to 1. Hence, the cubic corresponding to e_2 switches from C to C_Z. Since C_Z lies below C, $e_2(t)$ approaches $\mathcal{L}_Z$ during this inner solution.

The third piece of the singular solution is when e_1 is in its active phase, while e_2 is in its silent phase. During this time, $z = 1$. We need to choose the parameters so that e_1 reaches the right knee of C_Z before e_2 reaches the left knee. We do not want e_2 to jump up while e_1 is in its active phase. One way to do this is to choose the parameters so that the y-nullcline $\mathcal{H}$ intersects C_Z at a fixed point $p^Z = (x^Z, y^Z)$ along $\mathcal{L}_Z$, as shown in Fig. 7. This will guarantee that $e_2 \to p^Z$, and e_2 cannot jump up as long as e_1 is in its active phase. In Fig. 7, we show that e_1 reaches the right knee of C_Z at $t = t_2$.

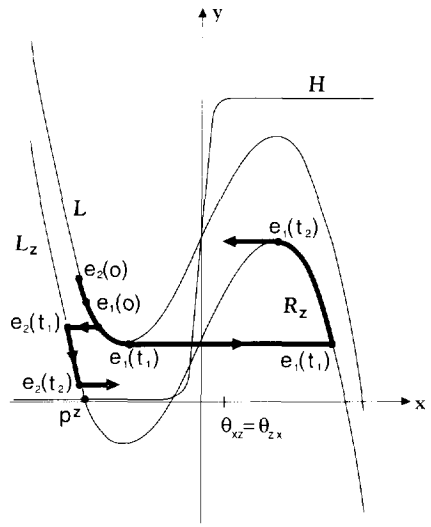

Fig. 7. Two oscillators coupled through global inhibition. When e_1 jumps up at time $t = t_1$, the cubic corresponding to e_2 lowers from C to C_Z. e_2 is not able to jump up until e_1 jumps down at $t = t_2$ and releases e_2 from the inhibition.

The fourth piece of the singular solution is when e_1 jumps down to the silent phase. When x_1 crosses θ_{zx}, σ_∞ switches from 1 to 0. Hence, z returns to 0 on the fast time scale. When z crosses θ_{xz}, $S_\infty(z, \theta_{xz})$ switches from 1 to 0. The cubic corresponding to e_2 then switches from C_Z to C. There are now two cases to consider. If e_2 lies below LK, as shown in Fig. 7, then e_2 jumps up immediately. The other case is if e_2 lies above LK. This results with e_1 and e_2 both lying on $\mathcal{L}$ and with e_2 below e_1. This new silent phase terminates when e_2 reaches LK and e_2 jumps up.

This example demonstrates the role of inhibition in desynchronizing the two oscillators. Even if e_1 and e_2 start very close to each other, once e_1 jumps up, e_2 is not able to jump up until e_1 returns to its silent phase. The threshold θ_{zx} acts as a gate in the sense that once e_1 crosses θ_{zx}, the inhibition is activated, or 'the gate is shut'. This lowers the cubic corresponding to e_2 on the fast time scale, thus preventing e_2 from jumping up. We demonstrate in the next section how to choose the parameters so that in the case of larger networks, oscillators within a given group representing the same pattern can 'pass through the gate', while oscillators not in the group are prevented from passing through. For this reason, we refer to this mechanism as *selective*

gating. In the next section, we show that once the two oscillators are separated in this way, they remain separated for all future time. The analysis generalizes to arbitrarily large populations of oscillators connected by a global inhibitor.

4. Analysis

4.1. Foreword

In this section, we prove a number of results concerning synchronization and desynchronization within the oscillator network. The first result is concerned with the synchronization of the oscillators within a given block. By a *block*, we mean the subset of oscillators whose input corresponds to some given pattern. In this model, a pattern will be a connected region. We prove that if the oscillators within a block begin sufficiently close to each other, then they will synchronize when jumping up to their active phases. The second main result is that there exists a singular solution of (2.1)–(2.4) in which different blocks remain separated. We show that if the blocks begin sufficiently far apart from each other, then they remain separated for all time. Moreover, at most one block can be in its active phase at any given time. Our final result is concerned with how blocks separate. For this result it will be necessary to make further assumptions on the connection weights. We prove that if all of the oscillators begin sufficiently close to each other, then after a fixed number of cycles the blocks will be separated. The analysis shows that if ϵ is sufficiently small, then the number of cycles required to reach full segmentation is no greater than the number of blocks.

We ignore all unstimulated oscillators in our analysis and assume that every oscillator is stimulated. The reason that we can do this without loss of generality, is the following. Recall that if e_i is an unstimulated oscillator, then $I_i = I^- < 0$. We choose the amplitude of the noise ρ and the weights $W_{ik}, k \in N(i)$, so that

$$I^- + \rho + \sum_{k \in N(i)} W_{ik} < 0$$

From our discussion of the single oscillator in the preceding section, it follows that there will always be a stable fixed point on the left branch of the cubic corresponding to e_i. Note that this cubic may change depending on the input that e_i receives. For example, e_i may sometimes receive input from the global inhibitor and sometimes it may not. In any case, e_i can never jump up to the right branch of a cubic, and it will not be able to oscillate. Hence, the unstimulated oscillators have no effect on the other oscillators.

In the following theorems, we consider the slow time scale. In particular, the inner solutions, during which times some oscillators make a rapid transition between the silent and active phases, are assumed to be instantaneous.

4.2. Synchronization of oscillators within a block

We now prove a result concerning the synchronization of the oscillators within one given block. This result states that the parameters in (2.1)–(2.4) can be chosen so that if all of the oscillators within a given block lie close enough to each other on the left branch of some cubic, then they will always jump up together, on the slow time scale. In this case, we refer to these oscillators as synchronized (cf. Subsection 4.4 for a more rigorous form of synchronization).

We assume throughout this section that $\mathcal{B}$ is a given block; it need not be the only block of oscillators. For convenience, we assume that when $t = 0$, all of the oscillators in $\mathcal{B}$ lie on either $\mathcal{L}$ or $\mathcal{L}_Z$. We also assume, without loss of generality, that $e_1 \in \mathcal{B}$, and if $e_j \in \mathcal{B}$, then $y_1(0) \leq y_j(0)$. Then e_1 is the first oscillator in $\mathcal{B}$ to jump up. Assume that this is at time t_0. Note that $y_1(t_0) \leq y_L$.

Proposition 4.2.1. Fix $M_0 > 0$ and $\Delta > 0$. The parameters in (2.1)–(2.4) can be chosen so that if e_j is any oscillator in $\mathcal{B}$ such that $\tau_L(y_1(0), y_j(0)) < M_0$, then $0 \leq y_j(t_0) - y_1(t_0) < \Delta$.

Proof. Note that if e_1 and e_j lie on the same left branch, say $\mathcal{L}$, for $0 < t < t_0$, then $\tau_L(y_1(t_0), y_j(t_0)) = \tau_L(y_1(0), y_j(0)) < M_0$. However, e_1 and e_j may jump back and forth between the left branches. This

is the case if there are other blocks besides $\mathcal{B}$. Since (SS) does not depend on the choice of left branch in the limit $\beta \to 0$, we can choose β sufficiently small so that if $\alpha \in \{L, Z\}$, then

$$\tau_\alpha(y_1(t_0), y_j(t_0)) < 2M_0 \tag{4.2.1}$$

We conclude the proof of the proposition by showing that given Δ, it is possible to choose the parameter I^+ so that if (4.1.1) is satisfied with $y_1(t_0) \le y_L$, then $y_j(t_0) - y_1(t_0) < \Delta$.

Choose I^* so that when $I^+ = I^*$, the y-nullcline $\mathcal{H}$ intersects C at the left knee LK. For this value of I^+, $\tau_L(y_L, y_j) = \infty$ for every $y_j > y_L$. Moreover, we can make $\tau_Z(y_L, y_j)$ as large as we please by choosing β small. It follows that for $\alpha \in \{L, Z\}$, $\tau_\alpha(y_1(t_0), y_1(t_0) + \Delta)$ can be made arbitrarily large by choosing $(I^+ - I^*)$ and β sufficiently small. In particular, we choose these parameters so that $\tau_\alpha(y_1(t_0), y_1(t_0) + \Delta) > 2M_0$. It follows that if $\tau_\alpha(y_1(t_0), y_j(t_0)) < 2M_0$, then $y_j(t_0) < y_1(t_0) + \Delta$, and this completes the proof. □

Theorem 4.2.2. Fix $M > 0$. The parameters in (2.1)–(2.4) can be chosen so that if $\tau_L(y_j, y_k) < M$ for each $e_j, e_k \in \mathcal{B}$ with $y_j \le y_k$, then all of the oscillators in $\mathcal{B}$ always jump up together, on the slow time scale.

Remark 4.2a. The theorem implies that if the oscillators in $\mathcal{B}$ begin sufficiently close to each other, then they always jump up at the same time. By 'sufficiently close' we mean that the time of excursion between any two oscillators is bounded. This bound can be made arbitrarily large by choosing the parameters appropriately. As we shall see, the 'time metric' is more natural for the statements and proofs of the theorems than the usual Euclidean metric. One reason for this is that as long as two oscillators remain on the same branch, the time metric between them remains invariant [1].

Proof. Let $\Delta_1 = Y_M - Y_Z$, $M_1 = \tau_L(Y_M - 3\Delta_1, Y_M)$, $M_0 = \max\{M, M_1\}$, and assume that $\Delta < y_m - y_L$. Choose the parameters so that Proposition 4.2.1 holds for this choice of M_0 and Δ. Then

$$y_j(t_0) < y_1(t_0) + \Delta < y_L + (y_m - y_L) = y_m$$

Hence, when e_1 jumps up at $t = t_0$, it causes its neighbors to jump up by fast threshold modulation. After a finite number of steps, every oscillator in $\mathcal{B}$ jumps up at $t = t_0$.

The oscillators in $\mathcal{B}$ move up their respective right branches until one of them reaches a right knee. Suppose that this happens when $t = t_1$. The rate at which each oscillator evolves during its active phase is determined by (SS_W) and depends on the particular cubic that the oscillator lies on. However, (2.1b) implies that $G_W(y) \to -y$ as $\beta \to 0$. Hence, the rates are independent of the cubic in the limit $\beta \to 0$. It follows that we can choose β and Δ sufficiently small so that when $t = t_1$, $\max\{|y_j - y_k| : e_j, e_k \in \mathcal{B}\} < \Delta_1$.

Once one oscillator in $\mathcal{B}$ jumps down to the silent phase, it causes the other oscillators in $\mathcal{B}$ to either jump down to the silent phase or fall down to the right branches of other cubics. In the latter case, the oscillators move up their new right branches before eventually jumping down. This causes the maximal distance between the oscillators to increase. However, the parameter γ controls the relative rates between when the oscillators evolve in the active phase and when they evolve in the silent phase. Choose t_2 so that the last oscillator in $\mathcal{B}$ jumps down to the silent phase at time t_2. If γ is sufficiently large, then we can guarantee that when $t = t_2$, $y_j > Y_M - 3\Delta_1$ for each $e_j \in \mathcal{B}$.

We now have that each oscillator in $\mathcal{B}$ lies on either $\mathcal{L}$ or $\mathcal{L}_Z$ with $Y_M - 3\Delta_1 < y_j(t_2) \le Y_M$. Hence, if e_j and e_k belong to $\mathcal{B}$ with $y_j(t_2) \le y_k(t_2)$ then

$$\tau_L(y_j(t_2), y_k(t_2)) < \tau_L(Y_M - 3\Delta_1, Y_M) \equiv M_1 \le M_0$$

By Proposition 4.2.1, when the oscillators in $\mathcal{B}$ jump up again,

$$\max\{|y_j - y_k| : e_j, e_k \in \mathcal{B}\} < \Delta < y_m - y_L$$

Hence, the oscillators in $\mathcal{B}$ all lie below LK_m and they jump up together. We can keep repeating this argument to show that the oscillators in $\mathcal{B}$ always jump up at the same time. □

[1] We are grateful to N. Kopell for pointing out the advantages of the time metric.

Remark 4.2b. Suppose that $M > 4M_1$. The proof of this theorem shows that if $\tau_L(y_j, y_k) < M$ for each $e_j, e_k \in \mathcal{B}$ with $y_j \leq y_k$, then, when the oscillators fall down after the first cycle, $\tau_L(y_j(t_2), y_k(t_2)) \leq M_1$ for each such e_j and e_k. Moreover, if β is sufficiently small, then $\tau_L(y_j(t), y_k(t)) < 2M_1 < M/2$ whenever $t > t_2$ and $\mathcal{B}$ lies in the silent phase. This gives some contraction on the dynamics which will be useful in Subsection 4.5.

4.3. Desynchronous solutions

For the following theorem, we assume that the blocks are initially separated. The theorem then implies that the blocks remain separated for all future time. That is, all of the oscillators within a given block jump up at the same (slow) time, the order in which the blocks jump up is fixed, and there is at most one block in the active phase at any given time. In the next section, we consider the case when all of the oscillators begin very close to each other. We prove that the blocks desynchronize (separate) after a fixed number of cycles. As before, we work on the slow time scale. Note that a block may consist of a single oscillator.

Theorem 4.3.1. We can choose the parameters in (2.1)–(2.4), $M > 0$, and a constant T^* so that the following holds. Assume that when $t = 0$, each oscillator lies on $\mathcal{L}$, and the hypotheses of Theorem 4.2.2 are satisfied for each block $\mathcal{B}$. If e_j and e_k belong to different blocks with $y_j \leq y_k$, assume that $\tau_L(y_j, y_k) > T^*$. Then there exists $T_0 > 0$ such that the singular solution of (2.1)–(2.4) satisfies the following:

(i) all of the oscillators within the same block jump up at the same (slow) time;
(ii) the ordering in which the blocks jump up is determined by their ordering on $\mathcal{L}$;
(iii) at least one block is in its active phase for some $t \in (0, T_0)$;
(iv) at most one block is in its active phase for any given $t \in (0, T_0)$;
(v) when $t = T_0$, all of the oscillators lie on $\mathcal{L}$, and the hypotheses of Theorem 4.2.2 are satisfied for each block $\mathcal{B}$. Moreover, if e_j and e_k belong to different blocks with $y_j \leq y_k$, then $\tau_L(y_j, y_k) > T^*$.

Remark 4.3a. The hypotheses of the theorem are still satisfied after time T_0. Hence, we may keep repeating the result to conclude that the blocks remain separated for all time.

Remark 4.3b. There is a natural ordering of the blocks on $\mathcal{L}$ at $t = 0$. This is because $\mathcal{L}$ is a one-dimensional curve, oscillators within a block begin very close to each other, and oscillators not in the same block begin bounded away from each other. The theorem then states that this natural ordering is preserved for all future time if the parameters are chosen appropriately. In particular, each block jumps up before any other block jumps twice. This may not remain true as the parameters are varied. In particular, we have numerically observed examples in which the ordering is not preserved if, for fixed values of the parameters, the number of blocks is too large.

Remark 4.3c. This theorem gives a global stability result. It implies that for a large class of initial data – namely, that given by the assumptions of the theorem – the corresponding solutions display the desired firing patterns in which the oscillators within a given block are synchronized and different blocks are separated from each other. This theorem is not a local result. It does not necessarily imply that there is a unique stable periodic solution of (2.1)–(2.4) whose basin of attraction is that given by the assumptions of the theorem. It is possible that the exact structure of stable periodic solutions, or even chaotic solutions, of (2.1)–(2.4) is quite complicated.

We begin the proof of Theorem 4.3.1 with two important technical results. For these results, we assume that e_1 and e_2 are any two oscillators in the network which both lie on $\mathcal{L}$ with $y_1 < y_2$. Choose t_0 so that $\psi_Z(y_1, t_0) = y_L$.

Proposition 4.3.2. If $0 < t \leq t_0$, then $\psi_Z(y_1, t) < \psi_L(y_1, t)$. Moreover,

(i) $\tau_Z(y_1, y_2) < \tau_L(y_1, y_2)$;

(ii) $\tau_Z(\psi_L(y_1,t),\psi_L(y_2,t))$ is a decreasing function of t;

(iii) $\tau_L(\psi_Z(y_1,t),\psi_Z(y_2,t))$ is an increasing function of t.

Proof. This is a restatement of [27, Proposition 2.3]. According to that result, the Proposition will follow once we show:

(a) $\partial g/\partial x > 0$ and $\partial g/\partial y < 0$ in the region between $\mathcal{L}_Z$ and $\mathcal{L}$,

(b) $(d/dy)[g(h(y),y) - g(h_Z(y),y)] < 0$ along $\mathcal{L}_Z$ and $\mathcal{L}$.

It is a simple matter to verify that these two conditions are satisfied for the nonlinearities defined in (3.1.1).□

Proposition 4.3.3. Given $\lambda \in (0,1)$, the parameters in (2.1)–(2.4) can be chosen so that $\lambda < \tau_Z(y_1,y_2)/\tau_L(y_1,y_2) < 1$ for all y_1, y_2 such that $y_L \le y_1 < y_2$.

Proof. It follows from the previous proposition that $h\tau_Z(y_1,y_2)/\tau_L(y_1,y_2) < 1$. Moreover, as $\beta \to 0, g(x,y) \to -y$. Therefore, in the limit $\beta \to 0, \tau_Z(y_1,y_2) = \tau_L(y_1,y_2)$. The result now follows if we assume that β is sufficiently small. □

In what follows, we assume that the conclusion of Proposition 4.3.3 is satisfied. The constant λ is chosen later.

We now return to the proof of Theorem 4.3.1. It is clear that each oscillator must jump up at some time. Moreover, by Theorem 4.2.2, all of the oscillators within a given block jump up at the same time. Recall that these oscillators need not jump down at the same time.

Denote the blocks by $\mathcal{B}_1, \mathcal{B}_2, \ldots, \mathcal{B}_{N_P}$ where N_P is the number of blocks. We assume, without loss of generality, that if $j < k$, $e_j \in \mathcal{B}_J$ and $e_k \in \mathcal{B}_K$, then $y_j(0) < y_k(0)$. We denote the subscripts for the blocks with capital letters, and a typical oscillator in that block with the corresponding lower case subscript. For example, we assume that $e_k \in \mathcal{B}_K$. Choose t_K so that each oscillator in $\mathcal{B}_K$ jumps up for the first time at $t = t_K$. Choose t^K and T^K so that during the first cycle, the first oscillator in $\mathcal{B}_K$ to jump down does so at $t = t^K$, while the last oscillator in $\mathcal{B}_K$ to jump down during this cycle does so at $t = T^K$. Hence, if $e_k \in \mathcal{B}_K$ then $e_k \in \mathcal{L} \cup \mathcal{L}_Z$ for $0 < t < t_K$, e_k lies on a right branch for $t_K < t < t^K$, and $e_k(t)$ jumps down to the silent phase for some $t \in [t^K, T^K]$.

It is possible that $t_K = T^J$ for $K \neq J$; that is, the oscillators in $\mathcal{B}_K$ jump up when an oscillator in $\mathcal{B}_J$ jumps down for the last time. In this case, there exists $e_k \in \mathcal{B}_K$, such that $e_k(T^J) \in \mathcal{L}_Z$ with $y_k(T^J) \le y_L$. In the proof that follows, we prove that there must exist some time when the last oscillator within some block jumps down, but no other oscillator jumps up. Define T_0 to be the first time at which this happens.

Let $T_R \equiv \tau_{W_m}(y_L, Y_m)$. We claim that given $\delta > 0$, we can choose the parameters so that for each K,

$$T_R - \delta < T^K - t_K < T_R + \delta \tag{4.3.1}$$

Recall that there is a fixed point of (SS_Z) at $p^Z = (x^Z, y^Z) \in \mathcal{L}_Z$. If an oscillator e_k jumps up at t_K and jumps down at $\hat{T}^K \in [t^K, T^K]$, then the proof of Theorem 4.2.2 demonstrates that

$$y^Z < y_k(t_K) < y_L + \Delta \quad \text{and}$$
$$|y_k(\hat{T}^k) - Y_m| < \Delta_1$$

where we can make Δ as small as is necessary by choosing the parameters appropriately. Note that we can make Δ_1 small by choosing the parameter W_M small. This gives a restriction on the connection weights. We choose the parameters so that

$$|\tau_W(y_k(t_K), y_L)| < \delta/3 \quad \text{and}$$
$$|\tau_W(y_k(\hat{T}^k), Y_m)| < \delta/3$$

for each $W \in [0, 4W_M]$. Moreover, the rates at which the oscillators evolve along the right branches are independent of which right branches the oscillators lie on in the limit $\beta \to 0$. Hence, if β is sufficiently small, then $|\tau_W(y_L, Y_m) - T_R| < \delta/3$ for each $W \in [0, 4W_M]$. From this, (4.3.1) follows. The constant δ is chosen later (see the sentence following (4.3.6)). Let

$$\delta_0 = \tau_Z(Y_M - 3\Delta_1, Y_M) \quad \text{and}$$
$$T^* = T_R - \delta - \delta_0. \tag{4.3.2}$$

The proof of Theorem 4.3.1 is now split into a number of lemmas. For each of these lemmas, we con-

sider singular solutions of (2.1)–(2.4). The results are shown to be true if the parameters are chosen appropriately. The first lemma is concerned with whether it is possible for more than one block to jump up when another block jumps down. The result implies that, under certain conditions, this is impossible.

Lemma 4.3.4. Suppose that there exists an integer $J \in [1, N_P - 2]$ such that for $1 \le K \le J$, $t_{K+1} = T^K$. Then $t_{K+2} > T^K$ for $1 \le K \le J$.

Remark 4.3d. Fix $K \in [1, J]$. It is clear that the ordering of the blocks in the silent phase is preserved for $0 < t < T^K$. Hence, the result implies that no blocks, except $\mathcal{B}_{K+1}$, jump up when the last oscillator in $\mathcal{B}_K$ jumps down.

Proof. Fix $K \in [1, J]$. Since $t_{K+1} = T^K$, there must exist $e_{k+1} \in \mathcal{B}_{K+1}$ with $y_{k+1}(T^K) \le y_L$. We need to prove that if $e_{k+2} \in \mathcal{B}_{K+2}$, then $y_{k+2}(T^K) > y_L$.

Let $T^0 = t_1$. Then some oscillator is active for each $t \in (T^0, T^K)$. Hence, $e_{k+2}(t) \in \mathcal{L}_Z$ if $t \in (T^0, T^K)$. We prove that $y_{k+2}(T^K) > y_L$ by showing that $\tau_Z(y_L, y_{k+2}(T^K)) > 0$. Note that

$$\tau_Z(y_L, y_{k+2}(T^K)) = \tau_Z(y_{k+1}(T^K), y_{k+2}(T^K)) - \tau_Z(y_{k+1}(T^K), y_L) \tag{4.3.3}$$

We estimate each term on the right-hand-side of (4.3.3). Since e_{k+1} and e_{k+2} both lie on $\mathcal{L}$ for $0 < t < T^0$, and both lie on $\mathcal{L}_Z$ for $T^0 < t < T^K$, it follows from Proposition 4.3.3 and the assumptions of the theorem that

$$\begin{aligned}
&\tau_Z(y_{k+1}(T^K), y_{k+2}(T^K)) \\
&\quad = \tau_Z(y_{k+1}(T^0), y_{k+2}(T^0)) \\
&\quad = \tau_L(y_{k+1}(T^0), y_{k+2}(T^0)) \\
&\qquad \times \frac{\tau_Z(y_{k+1}(T^0), y_{k+2}(T^0))}{\tau_L(y_{k+1}(T^0), y_{k+2}(T^0))} \\
&\quad = \tau_L(y_{k+1}(0), y_{k+2}(0)) \frac{\tau_Z(y_{k+1}(T^0), y_{k+2}(T^0))}{\tau_L(y_{k+1}(T^0), y_{k+2}(T^0))} \\
&\quad > \lambda T^* \qquad (4.3.4)
\end{aligned}$$

On the other hand, using (4.3.1), Proposition 4.3.3, and the assumptions of the theorem,

$$\begin{aligned}
&\tau_Z(y_{k+1}(T^K), y_L) \\
&\quad = \tau_Z(y_{k+1}(T^K), y_{k+1}(T^0)) - \tau_Z(y_L, y_{k+1}(T^0)) \\
&\quad = T^K - T^0 - \tau_Z(y_1(T^0), y_{k+1}(T^0)) \\
&\quad = T^K - T^0 - \sum_{j=1}^{K} \tau_Z(y_j(T^0), y_{j+1}(T^0)) \\
&\quad = T^K - T^0 - \sum_{j=1}^{K} \tau_L(y_j(T^0), y_{j+1}(T^0)) \\
&\qquad \times \frac{\tau_Z(y_j(T^0), y_{j+1}(T^0))}{\tau_L(y_j(T^0), y_{j+1}(T^0))} \\
&\quad \le T^K - T^0 - \lambda \sum_{j=1}^{K} \tau_L(y_j(T^0), y_{j+1}(T^0)) \\
&\quad \le K(T_R + \delta) - K\lambda T^* \qquad (4.3.5)
\end{aligned}$$

It follows from (4.3.3), (4.3.4), and (4.3.5) that

$$\begin{aligned}
&\tau_Z(y_L, y_{k+2}(T^K)) \\
&\quad > \lambda(K+1)T^* - K(T_R + \delta) \\
&\quad = \lambda(K+1)(T_R - \delta - \delta_0) - K(T_R + \delta)
\end{aligned}$$

The proof of the lemma will be complete if this last expression is positive. Since $K \le J \le N_P - 2$, it follows that $\tau_Z(y_L, y_{k+2}(T^K)) > 0$ if

$$\lambda > \left(\frac{N_P - 2}{N_P - 1}\right)\left(\frac{T_R + \delta}{T_R - \delta - \delta_0}\right) \tag{4.3.6}$$

From Proposition 4.3.2, we need to require that $\lambda < 1$. We can certainly choose $\lambda < 1$ so that (4.3.6) is satisfied if δ and δ_0 are sufficiently small. □

The following lemma implies that there exists some block such that when it jumps down to the silent phase, no other block jumps up.

Lemma 4.3.5. Suppose that $t_{K+1} = T^K$ for $1 \le K \le N_P - 1$. If $e_1 \in \mathcal{B}_1$, then $y_1(T^{N_P}) > y_L$.

Remark 4.3e. In the lemma, we assume that for $1 \le K \le N_P - 1$, $\mathcal{B}_{K+1}$ jumps up when $\mathcal{B}_K$ jumps down. The conclusion then states that, in this case, no block jumps up when $\mathcal{B}_{N_P}$ jumps down. Of course, if the hypothesis of the lemma is not satisfied, then there must certainly be some block such that when it jumps down to the silent phase, no other block jumps up.

Proof. We show that if the assumptions of the lemma are satisfied, then $\tau_Z(y_L, y_1(T^{N_P})) > 0$. We first estimate

$$\begin{aligned}&\tau_Z(y_L, y_1(T^{N_P-1}))\\&\quad=\tau_Z(y_{N_P}(T^{N_P-1}), y_1(T^{N_P-1}))\\&\quad-\tau_Z(y_{N_P}(T^{N_P-1}), y_L)\end{aligned}\tag{4.3.7}$$

Note that e_1 and e_{N_P} both lie on $\mathcal{L}_Z$ for $T^1 < t < T^{N_P-1}$. Moreover, the proof of Theorem 4.2.2 implies that $y_1(T^1) > Y_M - 3\Delta_1$. Hence, if $T_L \equiv \tau_Z(y_L, Y_M - 3\Delta_1)$, then

$$\begin{aligned}&\tau_Z(y_{N_P}(T^{N_P-1}), y_1(T^{N_P-1}))\\&\quad=\tau_Z(y_{N_P}(T^1), y_1(T^1))\\&\quad>\tau_Z(y_{N_P}(T^1), Y_M - 3\Delta_1)\\&\quad=\tau_Z(y_L, Y_M - 3\Delta_1) - \tau_Z(y_L, y_{N_P}(T^1))\\&\quad=T_L - \tau_Z(y_L, y_{N_P}(T^1))\end{aligned}\tag{4.3.8}$$

Since $y_{N_P}(T^{N_P-1}) \le y_L$, it follows as in (4.3.1) that

$$\begin{aligned}\tau_Z(y_L, y_{N_P}(T^1)) &\le T^{N_P-1} - T^1\\&\le (N_P - 2)(T_R + \delta)\end{aligned}$$

Together with (4.3.8), this implies that

$$\begin{aligned}&\tau_Z(y_{N_P}(T^{N_P-1}), y_1(T^{N_P-1}))\\&\quad> T_L - (N_P - 2)(T_R + \delta)\end{aligned}\tag{4.3.9}$$

On the other hand, (4.3.5), with $K = N_P - 1$, implies that

$$\begin{aligned}\tau_Z(y_{N_P}(T^{N_P-1}), y_L) &\le (N_P - 1)(T_R + \delta)\\&\quad-\lambda(N_P - 1)T^*\end{aligned}\tag{4.3.10}$$

It now follows from (4.3.7), (4.3.9), and (4.3.10) that

$$\begin{aligned}\tau_Z(y_L, y_1(T^{N_P-1})) &> T_L - (2N_P - 3)(T_R + \delta)\\&\quad+\lambda(N_P - 1)(T_R - \delta - \delta_0)\end{aligned}$$

Together with (4.3.6), this implies that

$$\tau_Z(y_L, y_1(T^{N_P-1})) > T_L - (N_P - 1)(T_R + \delta)$$

We assume that

$$T_L > N_P(T_R + \delta)\tag{4C.11}$$

This will be the case if the parameters γ is chosen sufficiently large and δ is sufficiently small. It then follows that $\tau_Z(y_L, y_1(T^{N_P-1})) > T_R + \delta$. From (4.3.1), $T^{N_P} - T^{N_P-1} < T_R + \delta$. Hence, $\tau_Z(y_L, y_1(T^{N_P})) > 0$, and the result follows. □

The following lemma completes the proof of Theorem 4.3.1. For this result, we identify $\mathcal{B}_1 \equiv \mathcal{B}_{N_P+1}$ and $\mathcal{B}_{N_P} \equiv \mathcal{B}_0$.

Lemma 4.3.6. Suppose that there exists $J \in [0, N_P]$ such that if $1 \le K < J$, then $t_{K+1} = T^K$. Moreover, assume that $t_{J+1} > T^J$. Then Theorem 4.3.1 follows with $T_0 = T^J$.

Remark 4.3f. In the statement of the lemma, J corresponds to the first block with the property that when it jumps down, no other block jumps up. In the preceding lemma, we proved that such a J exists.

Proof. Certainly when $t = T_0 \equiv T^J$, all of the blocks lie on $\mathcal{L}$ and their ordering is preserved for $0 < t < T_0$. Remark 4.2b demonstrates that the hypothesis of Theorem 4.2.2 are satisfied for each block if $M > 2M_1$. Moreover, by the previous lemmas, at most one block is in its active phase for $0 < t < T_0$, and at least one block, namely $\mathcal{B}_1$, did jump up during this time. So it remains to prove that if $e_k \in \mathcal{B}_K$ and $e_{k+1} \in \mathcal{B}_{K+1}$ then $\tau_L(y_k(T_0), y_{k+1}(T_0)) > T^*$ for all appropriate K.

We first assume that $J + 1 \le K \le N_P$. Then e_k did not jump up for $0 \le t \le T_0$. Since no oscillator is in its active phase for $0 < t < t_1 \equiv T^0$, it follows that

$$\tau_L(y_k(T^0), y_{k+1}(T^0)) = \tau_L(y_k(0), y_{k+1}(0)) > T^*$$

Moreover, there is always an oscillator in its active phase for $T^0 < t < T_0$. Hence, if we set $T_J = T_0 - T^0$, then

$$\begin{aligned}y_k(T_0) &= \psi_Z(y_k(T^0), T_J) \quad \text{and}\\y_{k+1}(T_0) &= \psi_Z(y_{k+1}(T^0), T_J)\end{aligned}$$

Therefore, by Proposition 4.3.2,

$$\begin{aligned}
&\tau_L(y_k(T_0), y_{k+1}(T_0)) \\
&\quad = \tau_L(\psi_Z(y_k(T^0), T_J), \psi_Z(y_{k+1}(T^0), T_J)) \\
&\quad > \tau_L(\psi_Z(y_k(T^0), 0), \psi_Z(y_{k+1}(T^0), 0)) \\
&\quad = \tau_L(y_k(T^0), y_{k+1}(T^0)) \\
&\quad > T^*
\end{aligned}$$

We now assume that $1 \le K \le J-1$. Then both e_k and e_{k+1} jumped up for $0 < t < T_0$. By (4.3.1), $s_K \equiv T^{K+1} - T^K > T_R - \delta$. Since $y_k(T^K) \le Y_M$,

$$y_k(T^{K+1}) = \psi_Z(y_k(T^K), s_K) < \psi_Z(Y_M, T_R - \delta)$$

or

$$\tau_Z(y_k(T^{K+1}), Y_M) > T_R - \delta$$

On the other hand, it follows from the proof of Theorem 4.2.2 and the definition of δ_0 given in (4.3.2) that

$$y_{k+1}(T^{K+1}) > Y_M - 3\Delta_1 = \psi_Z(Y_M, \delta_0)$$

This implies that

$$\tau_Z(y_{k+1}(T^{K+1}), Y_M) < \delta_0$$

Therefore,

$$\begin{aligned}
&\tau_Z(y_k(T^{K+1}), y_{k+1}(T^{K+1})) \\
&\quad = \tau_Z(y_k(T^{K+1}), Y_M) - \tau_Z(y_{k+1}(T^{K+1}), Y_M) \\
&\quad > T_R - \delta - \delta_0 \equiv T^*
\end{aligned}$$

Since e_k and e_{k+1} both lie on $\mathcal{L}_Z$ for $T^{K+1} < t < T_0$, it follows that

$$\begin{aligned}
\tau_Z(y_k(T_0), y_{k+1}(T_0)) &= \tau_Z(y_k(T^{K+1}), y_{k+1}(T^{K+1})) \\
&> T^*
\end{aligned}$$

Hence, by Proposition 4.3.2,

$$\begin{aligned}
\tau_L(y_k(T_0), y_{k+1}(T_0)) &> \tau_Z(y_k(T_0), y_{k+1}(T_0)) \\
&> T^*
\end{aligned}$$

It remains to consider the case $K = J$. However this is trivial since when $t = T_0$, $\mathcal{B}_J$ is the 'top' block on $\mathcal{L}$, while $\mathcal{B}_{J+1}$ is the 'bottom' block.

□

4.4. Separation of blocks

Our final result is concerned with how the blocks desynchronize themselves from each other. For this result, we need to make further assumptions on the connection weights. We do not state here the precise, detailed assumptions that are required for the proof. Instead, we consider a specific class of weights. After proving the theorem in this case, we discuss why the result extends to more general classes of connection weights.

Recently, Wang [51,52] proposed a mechanism called *dynamic normalization* to ensure that each oscillator, whether it is in the interior or on the boundary of the network, has equal overall connection weights from its neighbors. This mechanism uses a pair of connection weights from one oscillator j to another oscillator i, one permanent T_{ij}, and another dynamic J_{ij}. Permanent links reflect the hardwired structure of a network (2D grid), while dynamic links quickly change from time to time. In computations, though, only dynamic links formed on the basis of permanent links play an effective role. That is W_{ij} in (2.2) is set to J_{ij}. The idea of using two kinds of synaptic weights was first proposed by von der Malburg [48,50] who argued for its computational advantages and neurobiological plausibility (see also [7]). The dynamic normalization mechanism is adopted in the present model as a modification rule of dynamic links J_{ij} that combines a Hebbian rule [20] that emphasizes coactivation of oscillators i and j and a normalization of all incoming connections to an oscillator. More specifically, it is a two-step procedure: First update dynamic links and then normalization:

$$\begin{aligned}
\Delta J_{ij} &= \xi T_{ij} u(x_i) u(x_j) \\
J_{ij} &= W_A(J_{ij} + \Delta J_{ij}) / [c + \Sigma_k(J_{ik} + \Delta J_{ik})]
\end{aligned} \tag{4.4.1}$$

where ξ and W_A are both positive and the small constant c is introduced to prevent division by 0. In (4.4.1), ξ regulates the rate of modification and W_A specifies the overall connection strength to oscillator i. Function $u(x_i)$ measures whether oscillator i is activated by external stimulation. It is here simply

defined as $u(x) = 1$ if $\langle x \rangle$ is greater than a constant and $u(x) = 0$ otherwise. The angular bracket $\langle x \rangle$ stands for temporal averaging of the activity x over a period roughly corresponding to the period of oscillations. Each weight J_{ij} is updated once every step in the numerics. The outcome of (4.4.1) is that after an initial transient an effective connection is established between two oscillators if and only if they are neighbors and both of them are activated by external stimulation, and the overall dynamic weights to a single oscillator equal W_A. In engineering applications, however, J_{ij}'s can be properly set up in a single step at the beginning based on external stimulation. Notice that weight normalization is commonly used in neural network models for competitive learning [47,15].

In the previous section we showed that if the blocks begin sufficiently separated on $\mathcal{L}$, then they remain separated for all future time. We now assume that all of the oscillators begin close to each other on $\mathcal{L}$ and describe the segmentation process. Our analysis indicates that in the singular limit, the number of cycles required for full segmentation is no greater than the number of blocks. By one cycle, we mean the time for all of the oscillators to jump up exactly one time. For the following result, we assume dynamic normalization of the connection weights and consider singular solutions of (2.1)–(2.4). We also assume that each block consists of at least two oscillators. Then every oscillator receives some excitatory coupling while in the active phase. Notice that this assumption was not needed for our previous results. As before, we consider the slow time scale, and the result holds if the parameters are chosen appropriately.

Theorem 4.4.1. Fix $M > 0$. Suppose that when $t = 0$, all of the oscillators lie on $\mathcal{L}$ and $0 < \tau_L(y_j, y_k) < M$ for every e_j and e_k such that $y_j < y_k$. Then there exists $T > 0$ such that when $t = T$, the hypotheses of Theorem 4.3.1 are satisfied. That is, when $t = T$, all of the oscillators lie on $\mathcal{L}$, and the hypotheses of Theorem 4.2.2 are satisfied for each block $\mathcal{B}$. Moreover, if e_j and e_k belong to different blocks with $y_j \leq y_k$, then $\tau_L(y_j, y_k) > T^*$.

Remark 4.4a. The proof of this result demonstrates that T corresponds to no greater than N_P cycles where N_P is the number of blocks.

Remark 4.4b. We assume that no two oscillators begin at exactly the same position. This condition is only necessary if the oscillators lie in different blocks and is needed to avoid two oscillators in different blocks firing at exactly the same time. In this analysis, we are ignoring the role of noise in the model. It is clear that a small amount of noise will help to desynchronize the oscillators. Namely, if two oscillators within different blocks are, at some time, very close to each other, then because of the noise, the oscillators will, at some later time, be a small distance apart. This small distance may be enough to insure that the selective gating mechanism desynchronizes the oscillators.

Remark 4.4c. The assumption of normalized weights simplifies the analysis for the following reason. Recall that without this assumption, oscillators within the same block may lie on the right branches of different cubics in the active phase, and two oscillators within the same block need not jump down at the same (slow) time. With dynamic normalization, every oscillator within the same block receives the same input and hence lies on the same right branch during its active phase.

Suppose that W_A is the total connection strength to each oscillator in the active phase. We let $C_A = C(W_A, W_z)$. Here, we use the notation of Subsection 3.1. Let $\mathcal{R}_A$ denote the right branch of C_A and $RK_A = (X_A, Y_A)$ denote its right knee.

Proof. We show that after each cycle, at least one block breaks away from the rest of the oscillators. Hence, after N_P cycles, all of the blocks desynchronize from each other. It follows from Theorem 4.2.2 that the oscillators within each block remain synchronized.

As before, we denote the blocks by $\mathcal{B}_1, \mathcal{B}_2, \ldots, \mathcal{B}_{N_P}$, and assume that e_k is a typical oscillator in $\mathcal{B}_K$. We assume, without loss of generality, that $y_1(0) \leq y_j(0)$ if $j \neq 1$. Then $\mathcal{B}_1$ is the first block to jump up. Suppose that this happens at $t = t_1$. The oscillators in $\mathcal{B}_1$ then track along $\mathcal{R}_A$ until one of them reaches RK_A, say

at $t = T^1$. We claim that if the parameters are chosen appropriately, then all of the oscillators in $\mathcal{B}_1$ must fall down at T^1. By Proposition 4.2.1, given $\Delta > 0$, we can choose the parameters so that $y_L \le y_j(t_1) \le y_L + \Delta$ for all oscillators. A proof similar to that given in Theorem 4.2.2 demonstrates that Δ can be chosen so that if $\hat{e}_1 \in \mathcal{B}_1$, then $\hat{y}_1(T^1) > Y_A - W_m$. Hence, when $t = T^1$, each oscillator in $\mathcal{B}_1$ lies above the right knees of every cubic that corresponds to an input less than W_A. When e_1 jumps down, the inputs to e_1's neighbors in $\mathcal{B}_1$ decrease, and the cubics of these neighboring oscillators are then lowered. Since the neighbors in $\mathcal{B}_1$ lie above the right knees of the lowered cubics, these neighbors must jump down. In a similar fashion, the neighbors' neighbors must jump down at $t = T^1$. This continues until every oscillator in $\mathcal{B}_1$ jumps down to the silent phase.

Let $T_A = \tau_{W_A}(y_L, Y_A)$. We claim that given $\delta > 0$, we can choose the parameters so that

$$T_A - \delta < T^1 - t_1 < T_A \tag{4.4.2}$$

The proof of the first inequality is similar to that of (4.3.1). Actually this proof is easier than the proof of (4.3.1). In order to prove (4.3.1), we needed to assume that β is small, because previously, the oscillators may lie on different cubics in the active phase. This is not the case here. The second inequality follows because if $\hat{e}_1 \in \mathcal{B}_1$, then $y_L \le \hat{y}_1(t_1) < \hat{y}_1(T_1) \le Y_A$. Hence, $T^1 - t_1 \le \tau_{W_A}(y_L, Y_A) \equiv Y_A$.

Proposition 4.2.1 demonstrates that given $\Delta > 0$, we can choose the parameters so that $y_L \le y_j(t_1) < y_L + \Delta$ for all oscillators. Let $Y_0 \equiv \psi_Z(y_L + \Delta, T_A - \delta)$. Note that $Y_0 < y_L$ if Δ is sufficiently small. Hence, if $J \neq 1$ and $e_j \in \mathcal{B}_j$, then

$$\begin{aligned} y_j(T^1) &= \psi_Z(y_j(t_1), T^1 - t_1) < \psi_Z(y_L + \Delta, T_A - \delta) \\ &= Y_0 < y_L \end{aligned} \tag{4.4.3}$$

Therefore, when the last oscillator in $\mathcal{B}_1$ jumps down, all of the other blocks are released from inhibition and begin to jump up. It is possible that during this inner region, some of the blocks desynchronize themselves from the others. On the fast time scale, the oscillators which desynchronize themselves approach a right branch as $t \to \infty$, while the remaining blocks return to $\mathcal{L}_Z$ as $t \to \infty$. The reason that this can happen is the following.

Suppose that during this inner region, $e_j \in \mathcal{B}_J$ is the first oscillator to cross the line $x = \theta_{zx}$ while jumping up. We assume that θ_{zx} is chosen so that at this time, (x_j, y_j) must lie below the cubic $\mathcal{C}_Z$. See Fig. 7. When x_j crosses θ_{zx}, the inhibition is turned on again so that $z \to 1$. When z crosses θ_{xz}, the oscillators which lie above $\mathcal{C}_Z$ will 'turn around' and return to $\mathcal{L}_Z$. The other oscillators will jump up to the active phase. In particular, $\mathcal{B}_J$ will jump up.

Remark 4.4d. We do not use this mechanism for desynchronization in the proof, although it clearly enhances the process of desynchronization. Hence, the blocks may desynchronize in fewer than N_P cycles.

We consider the worst case. This is when all the blocks, except $\mathcal{B}_1$, jump up when $\mathcal{B}_1$ jumps down. These blocks then move up their right branches until one oscillator reaches RK_A, and that oscillator's block jumps down. Suppose that this block is $\mathcal{B}_2$ and it jumps down when $t = T^2$. Let $\sigma_0 \equiv \tau_{W_A}(Y_0, y_L)$. Then (4.4.3) implies that

$$T^2 - T^1 \ge T_A + \sigma_0 \tag{4.4.4}$$

Let e_1 be any oscillator in $\mathcal{B}_1$ and let e_j be any oscillator not in $\mathcal{B}_1$. We estimate $\tau_L(y_1(T^2), y_j(T^2))$. A proof similar to that given in Theorem 4.2.2 demonstrates that

$$y_j(T^2) > Y_A - \Delta \tag{4.4.5}$$

Moreover, since $y_1(T^1) \le Y_A$, (4.4.4) implies that

$$\begin{aligned} y_1(T^2) &= \psi_Z(y_1(T^1), T^2 - T^1) \\ &\le \psi_Z(Y_A, T_A + \sigma_0) \end{aligned} \tag{4.4.6}$$

It follows from (4.4.5), (4.4.6), and Proposition 4.3.2 that

$$\begin{aligned} &\tau_L(y_1(T^2), y_j(T^2)) \\ &\quad > \tau_L(\psi_Z(Y_A, T_A + \sigma_0), Y_A - \Delta) \\ &\quad > \tau_Z(\psi_Z(Y_A, T_A + \sigma_0), Y_A - \Delta) \\ &\quad = \tau_Z(\psi_Z(Y_A, T_A + \sigma_0), Y_A) - \tau_Z(Y_A - \Delta, Y_A) \end{aligned}$$

$$= T_A + \sigma_0 - \tau_Z(Y_A - \Delta, Y_A)$$
$$> T_A + \sigma_0/2$$

if Δ is sufficiently small.

This completes one cycle. Note that $\mathcal{B}_1$ has separated from the main group of oscillators, and every oscillator lies on $\mathcal{L}$. We now show that during the next cycle, some other block separates itself.

The next block to jump up is $\mathcal{B}_1$. Say that this is at $t = \hat{t}_1$. If $e_1 \in \mathcal{B}_1$ and $e_j \notin \mathcal{B}_1$, then

$$\tau_L(y_L, y_j(\hat{t}_1)) = \tau_L(y_1(T^2), y_j(T^2)) > T_A + \sigma_0/2$$

By Proposition 4.3.3, we can choose the parameters so that $\tau_Z(y_L, y_j(\hat{t}_1)) > T_A$.

We now claim that no oscillator jumps up when the oscillators in $\mathcal{B}_1$ jump down during this second cycle. Say that the oscillators in $\mathcal{B}_1$ jump down at $t = \hat{T}^1$. Then, as in (4.4.2), $\hat{T}^1 - \hat{t}_1 < T_A$. If $e_j \notin \mathcal{B}_1$, then

$$y_j(\hat{T}^1) = \psi_Z(y_j(\hat{t}_1), \hat{T}^1 - \hat{t}_1) > \psi_Z(y_j(\hat{t}_1), T_A)$$
$$> y_L$$

Therefore, every oscillator lies above the left knee of $\mathcal{L}$, and no oscillator jumps up when $\mathcal{B}_1$ jumps down. When the next oscillator jumps up, its block desynchronizes from the main group of oscillators. We now keep repeating the above argument to conclude that after each cycle, at least one new block separates itself from the rest. The above analysis also shows that after N_P cycles, the assumptions of Theorem 4.3.1 are satisfied. □

Remark 4.4e. It does not follow from our analysis that for arbitrary connection weights, the oscillators within a block reach complete synchronization, even in the singular limit. With normalized weights, however, we can prove that, in the singular limit, oscillators within a given block synchronize. That is, if the oscillators satisfy the assumptions of Theorem 4.2.2, then the maximal distance between any two oscillators in a block approaches zero. Moreover, the rate at which the oscillators approach synchrony is exponential. This follows because the normalized weight assumption implies that during both the silent and active phases, all of the oscillators within a block lie on the same branch of the same cubic. Moreover, they all jump up and jump down at the same time. During the silent and active phases, when the oscillators move along the same branch of a cubic, the maximal distance between the oscillators decreases at an exponential rate. This is complete synchronization; it is stronger than what is demonstrated in Subsection 4.2 where synchronization was taken to mean simultaneity in jumping up. Although we do not include a detailed proof of this result here, we will illustrate the result with numerical simulations in the next section.

Remark 4.4f. The proof of Theorem 4.4.1 demonstrates that there are at least two mechanisms for desynchronizing different blocks. The first mechanism is when every oscillator lies in its silent phase. When one oscillator reaches the left knee of $\mathcal{L}$, it jumps up and recruits the oscillators within its block, and, at the same time, prevents other blocks from jumping up by selective gating. This is the mechanism that was used in the proof of the theorem. The second mechanism was discussed in Remark 4.4d. In this case, oscillators of at least two blocks lie on $\mathcal{L}_Z$ below the left knee of $\mathcal{L}$. These oscillators begin to jump up at the same time when they are released from inhibition. If one of these oscillators crosses the threshold θ_{zx} sufficiently ahead of the oscillators in other blocks, then selective gating may prevent those blocks from jumping up. We did not use this second mechanism for desynchronization in the analysis. We expect that Theorem 4.4.1 holds for more general classes of connection weights besides those obtained by dynamic normalization. Numerical simulations, including those shown in the next section, clearly demonstrate that this is the case.

4.5. *Necessary assumptions on the nonlinearities and $\epsilon > 0$*

We never used the exact form of the nonlinear functions in (2.1)–(2.4) for the analysis. We now describe the assumptions necessary for the main theorems. We shall see that these results remain true for a large class of neural oscillators.

Assumptions on f and g are required in order that (a) and (b) in the proof of Proposition 4.3.2 to be

satisfied. Similar assumptions are required in Remark 4.4e. These conditions are not very restrictive; they follow for the nonlinearities in our model from simple conditions on the derivatives of f and g (see [27]).

Recall that in a singular solution, different oscillators may lie on the left or right branches of different cubics. It was important for our analysis that the dynamics on these branches does not depend heavily on the particular cubic. This was needed, for example, in the proof of Proposition 4.3.3 where we need that λ be close to one. We were able to guarantee that this is true by choosing the parameter β small. Note that a parameter similar to β appears in the Morris–Lecar model but not in the FitzHugh–Nagumo equations.

For the proof of Theorem 4.3.1, we need that (4.3.11) and (4.3.6) to be satisfied. These require that the time of excursion in the active phase is much shorter than the time of excursion in the silent phase. This condition is quite natural if we require that there be many blocks and only one block can be in its active phase at any time. We were able to satisfy this condition by choosing the parameter γ sufficiently large (see Fig. 3b). Note that δ and δ_0 depend on Δ_1 which depends on the choice of connection weights. Hence, in order for (4.3.6) and (4.3.11) to be satisfied, we must assume that the weights are not too large. If we assume weight normalization, then this restriction is not necessary.

All of the previous results are for singular solutions of (2.1)–(2.4) in which ϵ is formally set to zero. We conclude this section by showing how to extend the main theorems to the case when ϵ is positive. We begin with Theorem 4.3.1. Note that this includes Theorem 4.2.2. We prove that Theorem 4.3.1 remains valid for $\epsilon > 0$, except that the oscillators within a given block may not jump up at exactly the same time. The times at which they jump up will be very close to each other, however. In order to generalize Theorem 4.3.1 for ϵ positive, we must first extend the conclusion of the theorem in the following way.

The proof of Theorem 4.3.1 shows that there exists δ^* so that the theorem remains valid if we assume that at time $t = 0$, $y_i > y_L + \delta^*$ for each oscillator e_i. We may conclude that at $t = T_0$, $y_i > y_L + 2\delta^*$. Finally, in conclusion (5) of the theorem, we replace T^* with $T^* + \delta^*$.

We now reformulate the statement of Theorem 4.3.1 as follows. We view the solutions and singular solutions of (2.1)–(2.4) as trajectories in the full $(2N + 1)$-dimensional phase space where N is the number of oscillators. This is a slightly different point of view from what we took before. In our previous analysis, we often considered the two-dimensional phase space corresponding to each oscillator. Since, all of the oscillators are identical, we could project each of the oscillators onto the same two-dimensional phase space.

It is now necessary to define two subsets, $\mathcal{S}_0 \subset \mathcal{S}$, in the full phase space. We shall see that the singular flow defines a map from $\mathcal{S}$ into $\mathcal{S}_0$. Let M be as in Remark 4.2b. Define $\mathcal{S}$ to be the set of all points $(e_1, e_2, \ldots, e_N, z)$, where $e_j = (x_j, y_j)$, with the following properties:

(i) $y_L + \delta^* \le y_j \le Y_M + \delta^*$ for each oscillator;
(ii) if e_j and e_k belong to the same block with $y_j \le y_k$, then $\tau_L(y_j, y_k) < M$;
(iii) if e_j and e_k belong to different blocks and $y_j \le y_k$, then $\tau_L(y_j, y_k) > T^*$;
(iv) $|x_j - h(y_j)| < \delta^*$ for each oscillator;
(v) $|z| < \delta^*$.

We define $\mathcal{S}_0$ in a way similar to $\mathcal{S}$. Let $\mathcal{S}_0$ be the set of all points $(e_1, e_2, \ldots, e_N, z)$ with the following properties:

(i) $y_L + 2\delta^* \le y_j \le Y_M + \delta^*/2$ for each oscillator;
(ii) if e_j and e_k belong to the same block with $y_j \le y_k$, then $\tau_L(y_j, y_k) < M/2$;
(iii) if e_j and e_k belong to different blocks and $y_j \le y_k$, then $\tau_L(y_j, y_k) > T^* + \delta^*$;
(iv) $|x_j - h(y_j)| < \delta^*/2$ for each oscillator;
(v) $|z| < \delta^*/2$.

Note that $\mathcal{S}_0$ lies in the interior of $\mathcal{S}$. We show that the extension of Theorem 4.3.1 allows us to use the singular flow in order to define a map $\Phi_0 : \mathcal{S} \to \mathcal{S}_0$. Our previous analysis shows that this is true if each $e_k \in \mathcal{L}$. If $e_k = (x_k, y_k) \notin \mathcal{L}$, let $\pi(e_k) = (h(y_k), y_k) \in \mathcal{L}$. If $p = (e_1, \ldots, e_N, z) \in \mathcal{S}$, let $\Pi(p) = (\pi(e_1), \ldots, \pi(e_N), z)$. Then define $\Phi_0 : \mathcal{S} \to \mathcal{S}_0$ by $\Phi_0(p) = \Phi(\Pi(p))$.

We next extend Φ_0 to a map $\Phi_\epsilon : \mathcal{S} \to \mathcal{S}$ which depends continuously on ϵ for $\epsilon > 0$ sufficiently small. Fix $p \in \mathcal{S}$ and let $\psi_\epsilon(t)$ be the solution of (2.1)–

(2.4) with $\epsilon > 0$ and $\psi_\epsilon(0) = p$. Let $\psi_0(t)$ be the singular solution of (2.1)–(2.4) with $\psi_0(0) = p$. If $T > 0$ and $\mathcal{G}$ is any tubular neighborhood of $\psi_0(t)$, then $\psi_\epsilon(t) \in \mathcal{G}$ for $0 \leq t \leq T$ and ϵ sufficiently small (see [33]).

For each $p \in \mathcal{S}$, choose T_p so that $\Phi_0(p) = \psi_0(T_p) \in \mathcal{S}_0$. It follows that if ϵ is sufficiently small, then $\Phi_\epsilon(p) \equiv \psi_\epsilon(T_p) \in \mathcal{S}$, and $\psi_\epsilon(t)$ has the same 'firing pattern' as $\psi_0(t)$. Clearly, we can choose $\epsilon > 0$ so that this analysis holds for every $p \in \mathcal{S}$.

The extension of Theorem 4.3.1, and therefore Theorem 4.2.2, to the case $\epsilon > 0$ is now complete. We have demonstrated that for each $p \in \mathcal{S}$, there exists $T_p > 0$ such that $\psi_\epsilon(T_p) \in \mathcal{S}$. Moreover, ψ_ϵ shares the same firing pattern as ψ_0.

The proof of Theorem 4.4.1 extends to the case ϵ positive in a similar manner. If p is a point in the full phase space which satisfies the hypotheses of Theorem 4.4.1, then there must exist $T > 0$ such that $\psi_0(T) \in \mathcal{S}_0$. As before, this implies that $\psi_\epsilon(T) \in \mathcal{S}$ for $\epsilon > 0$ sufficiently small. We can then apply our extension of Theorem 4.3.1 to the case ϵ positive.

5. Computer simulation

To illustrate how the network architecture studied above can be used for scene segmentation, we have simulated a 20×20 grid of oscillators with a global inhibitor as defined by (2.1)–(2.4). For simplicity, each oscillator in this simulation was connected to its nearest neighbors by a constant weight, and W_{ik} in (2.2) was set to 2.5. To illustrate that dynamic normalization as assumed in Theorem 4.4.1 is not necessary for achieving segmentation, we did not use dynamic normalization in this simulation. we arbitrarily selected the scene in Fig. 1 as the input. This scene consists of three objects: the *sun*, a *tree*, and a *mountain*. These patterns were simultaneously presented to the grid as shown in Fig. 8a. Each pattern is a connected region, but no two patterns are connected to each other. All of the oscillators stimulated by the objects received an external input $I = 0.2$, while the unstimulated oscillators had $I = -0.02$ (see (2.1)). Thus the oscillators under stimulation were oscillatory, while those without stimulation remained silent. The amplitude ρ of the Gaussian noise was set to 0.02. Hence, compared to the external input, a 10% noise was included in every oscillator. We observed in the simulations that the noise facilitated the process of desynchronization.

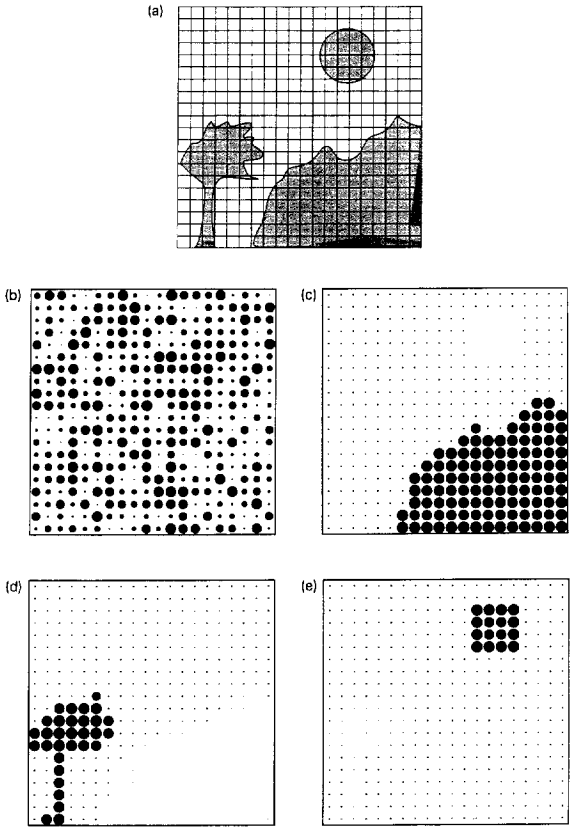

Fig. 8. Scene segmentation by an oscillator network. (a) The image shown in Fig. 1 is presented to a 20×20 grid of oscillators. Each square correponds to an oscillator. If a square is at least half covered by the image, the corresponding oscillator receives external input; otherwise, the corresponding oscillator receives no external input. (b) A snapshot of the activities of the oscillator grid at the beginning of dynamic evolution. (c) A snapshot of the activities of the oscillator grid shortly after the beginning. (d) Another snapshot taken shortly after (c). (e) Another snapshot taken shortly after (d).

The differential equations (2.1)–(2.4) were solved using both a fourth order Runge–Kutta method and the adaptive grid o.d.e. solver LSODE. For the simulation shown in Fig. 8, we chose the following values for the other parameters in (2.1)–(2.4): $\epsilon = 0.02$, $\phi = 3.0$, $\gamma = 6.0$, $\beta = 0.1$, $\kappa = 50$, $\theta_x = -0.5$, and $\theta_{zx} = \theta_{xz} = 0.1$.

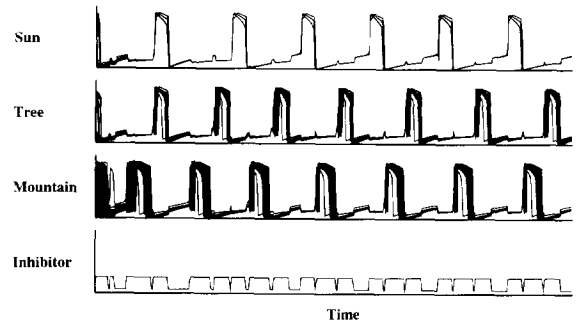

Fig. 9. Temporal activities of oscillator blocks. The upper three traces show the combined temporal activities of the oscillator blocks representing the patterns indicated by the symbols to their left, respectively. The bottom trace shows the temporal activity of the global inhibitor. The ordinate in the figure indicates the normalized x-activity of an oscillator calculated in the same way as in Fig. 8. The simulation took 8,000 integration steps.

The phases of all of the oscillators on the grid were randomly initialized. This simulation condition is more relaxed than what is assumed in the analysis where either the oscillators begin close to each other (Theorem 4.4.1) or the patterns are initially segmented (Theorem 4.3.1). The simulation results are displayed in Figs. 8 and 9. The diameter of each black circle represents the x-activity of the corresponding oscillator. That is, if the maximum and minimum x-values of all oscillators are x_{max} and x_{min}, respectively, then the diameter of the black circle corresponding to an oscillator is proportional to $(x-x_{min})/(x_{max}-x_{min})$.

Fig. 8b shows the instantaneous activity (snapshot) of the network a few steps after the beginning of the simulation. The activities of the oscillators at this time were largely random. Fig. 8c shows a snapshot after the system had evolved for a short time period. One can clearly see the effect of grouping and segmentation: all of the oscillators belonging to the *mountain* were entrained and had large activities. At the same time, the oscillators stimulated by the other two patterns had very small activities. Thus the *mountain* was clearly segmented from the rest of the input. A short time later, as shown in Fig. 8d, the oscillators stimulated by the *tree* reached their active phases and separated from the rest of the input. Finally, Fig. 8e shows that a short time later, the oscillators representing the *sun* were active while the rest of the input remained silent. This successive 'pop-out' of the objects continued in a stable periodic fashion as described in Theorem 4.3.1.

The patterns shown in Fig. 8a were completely segmented after just two cycles, and the segmentation process is consistent with that described by the analysis. This is best illustrated in Fig. 9 where we show the temporal evolution of each oscillator. Since the oscillators receiving no external input were inactive during the entire simulation process, they were excluded from the display in Fig. 9. The activities of the oscillators within each pattern (block) were combined together. Thus, if these oscillators are synchronized, then they appear like a single oscillator. In Fig. 9, the three upper traces represent the activities of the three oscillator blocks, and the bottom trace represents the activity of the global inhibitor. The synchronized oscillations within each object and desynchronization between the objects are clearly shown within two cycles of dynamic evolution.

The *mountain* popped out during the first cycle after initial random activation, but the synchronization within that pattern was weak as shown by the thick bundle of activity lines in jumping up. When the *mountain* returned to the silent phase and released the other oscillators from inhibition, the *sun* and the *tree* jumped up at approximately the same time.

During the second cycle, all of the three objects were separated. This state of segmentation is maintained in the following cycles, and the quality of synchrony within the *mountain* improved. In the figure, synchronization in jumping-up is not perfect even after several cycles, as shown by rather thick bundles particularly evident in the second and the third traces. But the quality of synchronization can be improved by reducing the value of ϵ. On the other hand, rather large discrepancies in jumping-down times are intrinsic in the model, and cannot be improved by varying ϵ. These numerical observations are consistent with the analysis of Section 4.

The process of scene segmentation is clearly indicated by the activity of the global inhibitor, which is activated if any oscillator on the grid reaches its active phase. As shown in Fig. 9, before segmentation is reached the time spans when the inhibitor is activated tend to be irregular. After segmentation is reached, the

time spans tend to be regularly spaced and their widths correspond to the time that a block stays in the active phase. As described in Section 3, the global inhibitor drove the oscillators representing different patterns to desynchronize.

As a comparison, we also simulated the same network for segmenting the same input by using dynamic weight normalization according to (4.4.1). Each oscillator forms a permanent link (T_{ij}) to its four nearest neighbors on the grid, except for those on the boundary where we assumed no wrap-up conditions. All permanent links were assumed to have the same strength (the precise value does not matter). A dynamic link J_{ij} is formed on the basis of T_{ij}, and dynamic normalization results in that only two neighboring oscillators stimulated by a single pattern have an effective dynamic connection. For total effective connections (see (4.4.1)) we set $W_A = 6.0$; the total dynamic weight to a single oscillator roughly corresponds to the total weights that an oscillator receives in the previous simulation shown in Fig. 8. The parameter ξ was set to 10. The values for the other parameters are the same as in the previous simulation, and the phase of every oscillator on the grid again was randomly initialized.

The simulation results are displayed in Fig. 10 in the same format as in Fig. 9. The network fully segmented all three objects in less than two cycles. After just two cycles, the synchrony within each pattern and desynchrony among the three patterns were almost perfect. Consistent with our discussion in Subsection 4.4, dynamic normalization also produces synchronization in jumping-down times within an oscillator block. Moreover, the simulation also reveals that the quality of synchronization in jump-up improves with dynamic normalization.

The exact shapes and positions of the patterns in Fig. 8 do not matter for scene segmentation using our approach. In fact, the two dimensional grid provides a general solution to segmentation of planar connected patterns. In addition to the simulations presented above, we have conducted many other simulation experiments with the model, and the results are as good as in Fig. 9 and Fig. 10. Furthermore, the results in all simulations that we conducted were robust with respect to considerable changes in the parameters of the model.

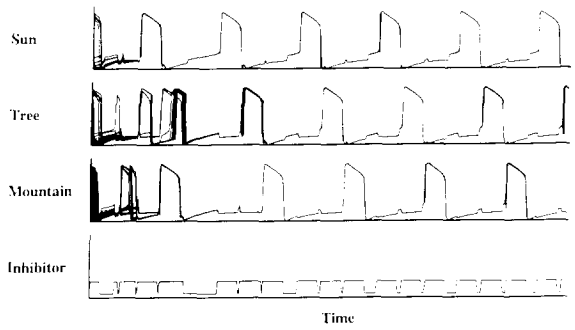

Fig. 10. Another simulation with dynamic normalization of connection weights. See the legend of Fig. 9 for explanations of this figure. As in Fig. 9, the simulation took 8,000 integration steps.

The network defined above can readily be applied to segmentation of binary images. For gray-level images (each pixel being in a certain value range), the following slight modification suffices to make the network applicable. An effective connection is established between two oscillators if and only if they are neighbors and the difference of their corresponding pixel values is below a certain threshold. This way, a homogeneous and connected region forms a segment, or a pattern, while boundaries among patterns are formed where a large gradient of pixel values is found. The latter condition underlies various algorithms of edge detection [41]. Formation of a single segment is, in a sense, an inverse process of finding closed contours, which emerge from gluing together nearby edge elements.

6. Discussion

As mentioned previously, the activity of a single oscillator can be interpreted either as the local field potential of a group of neurons or as the bursting behavior of a single neuron. The structure of our network model is also consistent with known neurobiology. Lateral connections, nearest neighbor connections being a special case, are one of basic structural characteristics of the brain [23]. The global inhibition may be interpreted as an attentional mechanism, possibly mediated by some subcortical areas such as the thalamus and/or the superior colliculus [7,8]. In particular, the thalamus sends its projections to and

receives input from much of the cortex, satisfying the structural requirements of the global inhibitor.

Besides neural plausibility, oscillatory correlation has a unique feature as a computational approach to the engineering of scene segmentation and figure/ground segregation. Due to the nature of oscillations, no single object can dominate and suppress the perception of the rest of the image permanently. The current dominant object has to give way to other objects being suppressed, and let them have a chance to be spotted. Although at most one object can be dominant at any time instant, due to rapid oscillations, a number of objects can be activated over a short time period. This intrinsic dynamic process provides a natural and reliable representation of multiple segmented patterns. With the selective gating mechanism, the utility of the representational advantage of oscillatory correlation is greatly enhanced. Other computational benefits of oscillatory correlation are further discussed in the following paragraphs.

In this paper, we have only studied synchrony and desynchrony of an oscillator network with nearest-neighbor connections. However, the basic principles of selective gating can be applied to networks with lateral connections beyond nearest neighbors. Indeed, in terms of synchronization, more distant connections even help expedite phase entrainment. In this sense, synchronization with all-to-all connections is a special case of our system. With lateral connections, we expect that the power of the network would be markedly increased for scene segmentation. With nearest-neighbor connectivity (Fig. 4), any isolated part of an image is considered as a segment. In a noisy image with many tiny regions, segmentation would result in too many small fragments. More distant connections would provide a solution to this problem. Lateral connections may take on the typical form of a Gaussian distribution, with the connection strength between two oscillators falling off exponentially. Since global inhibition is superimposed onto local excitation, two oscillators positively coupled may still be desynchronized if global inhibition is strong enough. Thus, it is unlikely that all objects in an image form a single segment as a result of extended connections, an undesirable situation contrary to the problem of fragmentation.

The prototype of our analysis and simulation is a 2-D oscillator network. However, the results are also applicable to networks of other dimensions. This is because, in the analysis, we speak of only oscillator blocks which are formed by local connections, without specific reference to the dimension of the network. Thus, one can easily extend the analysis to other dimensions as well.

In one of the first studies of using a laterally connected oscillator network to achieve scene segmentation, Sporns et al. [46] simulated a large neural network with four layers, each having 16×16 groups of neurons. Each group has 60 neurons and behaves as a single oscillator. Four layers process four directions of movement respectively. Obviously, this model is computationally expensive. As discussed in Section 1, the lack of a desynchronization mechanism requires the model to take averaging of multiple trials in order to achieve the segmentation of different patterns, further increasing the computational demand. They demonstrated synchrony beyond the range of direct connections, but it is not clear from their simulation whether synchrony can be maintained for a much larger range beyond direct connections. Their use of different layers to process different directions of movement, however, provides a promising framework to address segmentation based on motion. This idea can be furthered to accommodate different orientations of curve segments. With inclusion of orientation sensitivity and directional sensitivity, two basic properties of the visual system, our network should be able to model a variety of grouping phenomena in vision and to provide an effective algorithm for various scene segmentation tasks.

Our result of global synchrony emerging from only local coupling appears in contradiction with the well-known theorem of Mermin and Wagner [31] in statistical mechanics. The theorem states that no long-range order (synchrony) exists in one- or two-dimensional isotropic Heisenberg models (X-Y models). The fact that our system is not an equilibrium statistical mechanical system makes it not subject to the theorem. We also note that our relaxation oscillators are far from being isotropic. This is incompatible with the condi-

tion of isotropy of the Mermin and Wagner theorem [2]. On the other hand, sinusoidal oscillators as widely used by many others (see, for example, [6]) to model phase synchrony tend to be isotropic and are probably subject to the theorem. This might explain why long range connections have to be used in these models in order to reach global network synchronization. Somers and Kopell [43] and Wang [51,52] have also realized the qualitative differences in synchronization behaviors between sinusoidal and relaxation oscillators. Our analysis further demonstrates that different models of single oscillators may lead to qualitatively different global behaviors.

The rigorous analysis in Section 4 demonstrates that pattern formation is a robust property of the model; it exists for a large class of initial data and it is not sensitive to moderate changes of the parameters. The analysis explains why scene segmentation is an intrinsic property of the model and indicates how parameters should be chosen to achieve scene segmentation. The analysis also indicates how instabilities can arise as the parameters are varied. The proof of Theorem 4.2.2, for example, demonstrates that the oscillators within a given pattern may not synchronize if the parameter γ is too small.

As discussed in Subsection 4.5, the analysis applies to a general class of models which includes (2.1)–(2.4). For this reason, it helps to explain why some models, such as the conductance based, single-cell model of Morris and Lecar, are more appropriate for scene segmentation than other models, such as the FitzHugh–Nagumo model. In [43] there is a discussion as to why fast threshold modulation in relaxation-type oscillators is advantageous to the push-pull mechanism in phase models for achieving rapid synchronization within one pattern.

The analysis helps to explain why some choices for connection weights are advantageous over others. In Subsection 4.4, we discussed why the dynamic normalization mechanism helps in the synchronization of oscillators within a single block and the desynchronization between different blocks. The proof of the Theorem 4.4.1 also demonstrates how instabilities may arise for other choices of connection weights.

Another reason why the analysis is important is because networks of coupled oscillators often lead to very complex and surprising behaviors. For example, one may naively think that identical oscillators coupled through mutual excitation will always lead to synchrony. It is demonstrated in [27], however, that it is possible for this simple network to give rise to anti-phase solutions. On the other hand, it is often assumed that identical oscillators coupled through mutual inhibition will always lead to anti-phase solutions. It is demonstrated in [56] that if the inhibition decays at a sufficiently slow rate, then the synchronous solution may be stable.

We have demonstrated that the theorems in Section 4 extend to the case $\epsilon > 0$ sufficiently small. How small ϵ must be, however, may depend on the number of oscillators. It is not clear, for example, how the number of cycles needed for scene segmentation depends on the number of oscillators if ϵ is positive. Our analysis shows that the number of cycles only depends on the number of patterns if ϵ is sufficiently small. We conjecture that this remains true if $\epsilon = \mathcal{O}(1/N)$ where N is the number of oscillators.

The analysis indicates that for a given set of parameters, there is an upper bound on the number of blocks which can be segmented. The inequality (4.3.11), for example, gives an upper bound on the number of patterns in terms of the time of excursion along the right and left branches of the cubics. Our results state that for a given number of patterns, no matter how large, it is possible to choose the parameters so that the given patterns will be segmented. However, once we fix the parameters, the number of patterns cannot be arbitrarily large. This limitation of our system on the number of patterns that can be segmented seems consistent with the well-known psychological result that humans have fundamental limits on the number of objects that can be held in their attentional span [32].

Due to its critical importance for computer vision, scene segmentation, or perceptual organization as known in computer vision, has been studied quite extensively. Many techniques have been proposed in the past (for reviews of the subject see [29,19,40]).

[2] We are grateful to J. Cheyes and C. Jayaprakash who helped us realize the applicability of the Mermin and Wagner theorem.

Despite these techniques, as pointed out by Haralick and Shapiro [19], there is no underlying theory of image segmentation, and the techniques tend to be ad hoc and emphasize some aspects while ignoring others. One such technique is based on thresholding. The basic idea of thresholding is that a pixel is assigned a specific label if some measure of the pixel passes a certain threshold. This idea can be extended to a complex form including multiple thresholds [25]. This way, a region of pixels are grouped together if their measurements fall between two threshold values. Another popular technique is region growing (or similarly region splitting, see [21,41]), where iterative steps are taken to grow a seed pixel into a connected region if all the pixels in the region satisfy some condition. One such condition is that the distance between the minimum and the maximum pixel values is within a pre-defined range. Most of the techniques use one or more Gestalt principles of perceptual grouping that emphasize spatial and temporal relationships among object components [34,40]. Gestalt grouping principles, such as connectedness and proximity, were derived from the studies of human visual perception by Gestalt psychologists [24,39]. One of the apparent deficits with these algorithms lies in their iterative (serial) nature [28]. There are some recent algorithms which are partially parallel. In Sha'ashua and Ullman [42], a globally consistent curve structure is detected using a locally connected network. In Liou et al. [28], a parallel technique is used to search a partition space. In Mohan and Nevatia [34], part of the segmentation process is performed by a neural network for cost optimization.

Compared to the above techniques for scene segmentation, the oscillatory correlation approach offers many unique advantages. The dynamic process is inherently parallel. Each single oscillator behaves fully in parallel with all of the others in the network. This feature is particularly attractive in the context that an image generally consists of many pixels (256×256), and the current technology of computer architecture can support massive parallel computations. While conventional computer vision algorithms are based on descriptive criteria and many ad hoc heuristics, the network architecture such as the one shown in Fig. 4 performs computations based on only connections and oscillatory dynamics. The organizational simplicity renders the oscillator network particularly feasible for VLSI chip implementation. Also, continuous time dynamics allows real time processing as desired by many engineering applications.

Neural oscillations have been demonstrated not only in vision but also in other sensory modalities, including audition [14,30] and olfaction [13] (for modeling, see [2]). With its computational properties plus the support of biological evidence, oscillatory correlation promises to offer a general computational theory for scene segmentation and figure/ground segregation (see also Wang [54] for a study in audition).

7. Conclusion

We have proposed and analyzed a network of neural oscillators with local excitation and global inhibition. The mechanism of selective gating leads the network to form blocks of locally cooperative oscillators which are stimulated by external input. Within each block neural oscillators synchronize with each other, and each block separates itself in phase from all the other blocks. This state of oscillatory dynamics is proven to be globally stable. The analysis demonstrates how parameters in the model should be chosen to achieve scene segmentation and why some models are more advantageous to others. The mechanism of selective gating provides a physical foundation for the theory of oscillatory correlation. Computer simulations have been conducted to demonstrate scene segmentation based on the mechanism. We have argued that the mechanism is biologically plausible and may provide a general framework for effective automatic scene segmentation and figure/ground segregation.

Acknowledgements

The first author is supported in part by the NSF grant DMS-9203299LE. The second author is supported in part by the NSF grant IRI-9211419 and the ONR grant N00014-93-1-0335.

References

[1] M. Abeles, Local Cortical Circuits (Springer, New York, 1982).

[2] B. Baird, Nonlinear dynamics of pattern formation and pattern recognition in the rabbit olfactory bulb, Physica D 22 (1986) 150–175.

[3] P. Baldi and R. Meir, Computing with arrays of coupled oscillators: An application to preattentive texture discrimination, Neural Comput. 2 (1990) 458–471.

[4] J. Buhmann, Oscillations and low firing rates in associative memory neural networks, Phys. Rev. A 40 (1989) 4145–4148.

[5] T. Chawanya, T. Aoyagi, I. Nishikawa, K. Okuda, and Y. Kuramoto, A model for feature linking via collective oscillations in the primary visual cortex, Biol. Cybern. 68 (1993) 483–490.

[6] A.H. Cohen, P.J. Holmes and R.H. Rand, The nature of coupling between segmental oscillators, of the lamprey spinal generator for locomotion: A mathematical model J. Math. Biol. 13 (1982) 345–369.

[7] F. Crick, Function of the thalamic reticular complex: The searchlight hypothesis, Proc. Natl. Acad. Sci. USA 81 (1984) 4586–4590.

[8] F. Crick and C. Koch, Towards a neurobiological theory of consciousness, Sem. Neurosci. 2 (1990) 263–275.

[9] R. Eckhorn, R. Bauer, W. Jordan, M. Brosch, W. Kruse, M. Munk and H.J. Reitboeck, Coherent oscillations: A mechanism of feature linking in the visual cortex?, Biol. Cybern. 60 (1988) 121–130.

[10] A.K. Engel, P. König, A.K. Kreiter and W. Singer, Synchronization of oscillatory neuronal responses between striate and extrastriate visual cortical areas of the cat, Proc. Natl. Acad. Sci. USA 88 (1991) 6048–6052.

[11] A.K. Engel, P. König, A.K. Kreiter and W. Singer, Interhemispheric synchronization of oscillatory neuronal responses in cat visual cortex, Science 252 (1991) 1177–1179.

[12] R. FitzHugh, Impulses and physiological states in models of nerve membrane, Biophys. J. 1 (1961) 445–466.

[13] W.J. Freeman, Spatial properties of an EEG event in the olfactory bulb and cortex, Electroencephalogr. Clin. Neurophysiol. 44 (1978) 586–605.

[14] R. Galambos, S. Makeig and P.J. Talmachoff, A 40-Hz auditory potential recorded from the human scalp, Proc. Natl. Acad. Sci. USA 78 (1981) 2643–2647.

[15] G.J. Goodhill and H.G. Barrow, The role of weight normalization in competitive learning, Neural Comput. 6 (1994) 255–269.

[16] E.R. Grannan, D. Kleinfeld and H. Sompolinsky, Stimulus-dependent synchronization of neuronal assemblies, Neural Comput. 5 (1993) 550–569.

[17] C.M. Gray, P. König, A.K. Engel and W. Singer, Oscillatory responses in cat visual cortex exhibit inter-columnar synchronization which reflects global stimulus properties, Nature 338 (1989) 334–337.

[18] S. Grossberg and D. Somers, Synchronized oscillations during cooperative feature linking in a cortical model of visual perception, Neural Networks 4 (1991) 453–466.

[19] R.M. Haralick and L.G. Shapiro, Image segmentation techniques, Comput. Graphics Image Process. 29 (1985) 100–132.

[20] D.O. Hebb, The Organization of Behavior (Wiley, New York, 1949).

[21] S.L. Horowitz and T. Pavlidis, Picture segmentation by a tree traversal algorithm, J. ACM 23 (1976) 368–388.

[22] D.M. Kammen, P.J. Holmes and C. Koch, Origin of oscillations in visual cortex: Feedback versus local coupling, in: Models of Brain Functions, R.M.J. Cotterill, ed., (Cambridge Univ. Press, Cambridge, 1989) 273–284.

[23] E.R. Kandel, J.H. Schwartz and T.M. Jessell, Principles of Neural Science, 3rd Ed. (Elsevier, New York, 1991).

[24] K. Koffka, Principles of Gestalt Psychology (Harcourt, New York, 1935).

[25] R. Kohler, A segmentation system based on thresholding, Comput. Graphics Image Process 15 (1981) 319–338.

[26] P. König and T.B. Schillen, Stimulus-dependent assembly formation of oscillatory responses: I. Synchronization, Neural Comput. 3 (1991) 155–166.

[27] N. Kopell and D. Somers, Anti-phase solutions in relaxation oscillators coupled through, excitatory interactions, J. Math. Biology (1994), to appear..

[28] S.P. Liou, A.H. Chiu and R.C. Jain, A parallel technique for signal-level perceptual organization, IEEE Trans. Patt. Anal. Machine Intell. 13 (1991) 317–325.

[29] D.G. Lowe, Perceptual Organization and Visual Recognition (Kluwer Academic, Boston, 1985).

[30] C. Madler and E. Pöppel, Auditory evoked potentials indicate the loss of neuronal, oscillations during general anesthesia Naturwissenschaften 74 (1987) 42–43.

[31] N.D. Mermin and H. Wagner, Absence of ferromagnetism or antiferromagnetism in one- or two- dimensional isotropic Heisenberg models, Phys. Rev. Lett. 17 (1966) 1133–1136.

[32] G.A. Miller, The magical number seven, plus or minus two: some limits on our capacity for processing information, Psychol. Rev. 63 (1956) 81–97.

[33] E.F. Mishchenko and N.Kh. Rozov, Differential Equations with Small Parameters and Relaxation Oscillations (Plenum Press, New York, London, 1980).

[34] R. Mohan and R. Nevatia, Perceptual organization for pattern segmentation and description, IEEE Trans. Patt. Anal. Machine Intell. 14 (1992) 616–635.

[35] C. Morris and H. Lecar, Voltage oscillations in the barnacle giant muscle fiber, Biophys. J. 35 (1981) 193–213.

[36] T. Murata and H. Shimizu, Oscillatory binocular system and temporal segmentation of stereoscopic depth surfaces, Biol. Cybern. 68 (1993) 381–390.

[37] V.N. Murthy and E.E. Fetz, Coherent 25- to 35-Hz oscillations in the sensorimotor cortex of awake behaving monkeys, Proc. Natl. Acad. Sci. USA 89 (1992) 5670–5674.

[38] J. Nagumo, S. Arimoto and S.Yoshizawa, An active pulse transmission line simulating nerve axon, Proc. IRE. 50 (1962) 2061–2070.

[39] I. Rock and S. Palmer, The legacy of Gestalt psychology, Sci. Am. 263 (1990) 84–90.

[40] S. Sarkar and K.L. Boyer, Perceptual organization in computer vision: a review and a proposal for a classificatory structure, IEEE Trans. Syst. Man Cybern. 23 (1993) 382–399.

[41] R. Schalkoff, Digital Image Processing and Computer Vision (Wiley, New York, 1989).

[42] A. Sha'ashua and S. Ullman, Structural saliency: The detection of globally salient structures using a locally connected network, Proc. Int. Conf. Comput. Vision (1988) 321–327.

[43] D. Somers and N. Kopell, Rapid synchronization through fast threshold modulation, Biol. Cybern 68 (1993) 393–407.

[44] H. Sompolinsky, D. Golomb and D. Kleinfeld, Cooperative dynamics in visual processing, Phys. Rev. A 43 (1991) 6990–7011.

[45] O. Sporns, J.A. Gally, G.N. Reeke Jr. and G.M. Edelman, Reentrant signaling among simulated neuronal groups leads to coherency in their oscillatory activity, Proc. Natl. Acad. Sci. USA 86 (1989) 7265–7269.

[46] O. Sporns, G. Tononi and G.M. Edelman, Modeling perceptual grouping and figure-ground segregation by means of active reentrant connections, Proc. Natl. Acad. Sci. USA 88 (1991) 129–133.

[47] C. von der Malsburg, Self-organization of orientation sensitive cells in the striate cortex, Kybernetik 14 (1973) 85–100.

[48] C. von der Malsburg, The Correlation Theory of Brain Functions, Internal Report 81–2, Max-Planck-Institut for Biophysical Chemistry, Göttingen, FRG (1981).

[49] C. von der Malsburg and J. Buhmann, Sensory segmentation with coupled neural oscillators, Biol. Cybern. 67 (1992) 233–246.

[50] C. von der Malsburg and W. Schneider, A neural cocktail-party processor, Biol. Cybern. 54 (1986) 29–40.

[51] D.L. Wang, Modeling global synchrony in the visual cortex by locally coupled neural oscillators, Proc. 15th Ann. Conf. Cognit. Sci. Soc. (1993) 1058–1063.

[52] D.L. Wang, Emergent synchrony in locally coupled neural oscillators, IEEE Trans. Neural Networks 6 (1995), in press.

[53] D.L. Wang, Pattern recognition: Neural networks in perspective, IEEE Expert 8 (1993) 52–60.

[54] D.L. Wang, An oscillatory correlation theory of temporal pattern segmentation, in: Neural Representation of Temporal Patterns, E. Covey, H. Hawkins, T. McMullen and R. Port, eds., (Plenum, New York, 1995), to appear.

[55] D.L. Wang, J. Buhmann and C. von der Malsburg, Segmentation in associative memory, Neural Comput. 2 (1990) 94–106.

[56] X.J. Wang and J. Rinzel, Alternating and synchronous rhythms in reciprocally inhibitory model neurons, Neural Comput. 4 (1992) 84–97.